

Discriminating $B \rightarrow D^*\ell\nu$ form factors via polarization observables and asymmetries

Marco Fedele^{1,*} Monika Blanke,^{1,2,†} Andreas Crivellin,^{3,4,‡} Syuhei Iguro,^{1,2,§} Ulrich Nierste^{1,||}, Silvano Simula^{5,¶} and Ludovico Vittorio^{6,**}

¹*Institut für Theoretische Teilchenphysik (TTP), Karlsruhe Institute of Technology,
D-76131 Karlsruhe, Germany*

²*Institut für Astroteilchenphysik (IAP), Karlsruhe Institute of Technology,
D-76344 Eggenstein-Leopoldshafen, Germany*

³*Paul Scherrer Institut, CH-5232 Villigen PSI, Switzerland*

⁴*Physik-Institut, Universität Zürich, Winterthurerstrasse 190, 8057 Zürich, Switzerland*

⁵*Istituto Nazionale di Fisica Nucleare, Sezione di Roma Tre, Via della Vasca Navale 84,
I-00146 Rome, Italy*

⁶*LAPTh, Université Savoie Mont-Blanc and CNRS, F-74941 Annecy, France*



(Received 5 June 2023; accepted 12 September 2023; published 29 September 2023)

Form factors are a crucial theory input in order to extract $|V_{cb}|$ from $B \rightarrow D^{(*)}\ell\nu$ decays, to calculate the Standard Model prediction for $\mathcal{R}(D^{(*)})$ and to assess the impact of new physics. In this context, the dispersive matrix approach, a first-principle calculation of the form factors, using no experimental data but rather only lattice QCD results as input, was recently applied to $B \rightarrow D^{(*)}\ell\nu$. It predicts (within the Standard Model) a much milder tension with the $\mathcal{R}(D^*)$ measurements than the other form factor approaches, while at the same time giving a value of $|V_{cb}|$ compatible with the inclusive value. However, this comes at the expense of creating tensions with differential $B \rightarrow D^*\ell\nu$ distributions (with light leptons). In this article, we explore the implications of using the dispersive matrix method form factors, in light of the recent Belle (II) measurements of the longitudinal polarization fraction of the D^* in $B \rightarrow D^*\ell\nu$ with light leptons, F_L^ℓ , and the forward-backward asymmetry, A_{FB}^ℓ . We find that the dispersive matrix approach predicts a Standard Model value of F_L^ℓ that is in significant tension with these measurements, while mild deviations in A_{FB}^ℓ appear. Furthermore, F_L^ℓ is very insensitive to new physics such that the latter cannot account for the tension between dispersive matrix predictions and its measurement. While this tension can be resolved by deforming the original dispersive matrix form factor shapes within a global fit, a tension in $\mathcal{R}(D^*)$ reemerges. As this tension is milder than for the other form factors, it can be explained by new physics not only in the tau lepton channel but also in the light lepton modes.

DOI: 10.1103/PhysRevD.108.055037

I. INTRODUCTION

Due to the chiral suppression of purely leptonic B decays, the most precise direct determinations of the

Cabibbo-Kobayashi-Maskawa (CKM) matrix element $|V_{cb}|$ originate from semileptonic B decays [1–12]. However, the exclusive and inclusive determinations of $|V_{cb}|$ have been in tension with each other for a long time now [12,13]. Furthermore, the exclusive value is also in tension with the indirect determination of $|V_{cb}|$ from the unitarity triangle analysis [14,15], which points toward its inclusive value. As this inclusive/exclusive discrepancy cannot be explained by physics beyond the Standard Model (SM) [16–18],¹ scrutiny of the different theoretical methods is even more important.

^{*}marco.fedele@kit.edu
[†]monika.blanke@kit.edu
[‡]andreas.crivellin@cern.ch
[§]igurosyuhei@gmail.com
^{||}ulrich.nierste@kit.edu
[¶]silvano.simula@roma3.infn.it
^{**}ludovico.vittorio@lapth.cnrs.fr

Published by the American Physical Society under the terms of the [Creative Commons Attribution 4.0 International license](#). Further distribution of this work must maintain attribution to the author(s) and the published article's title, journal citation, and DOI. Funded by SCOAP³.

¹Previously, an explanation via a right-handed charged current was possible [19]. However, with the recent exclusive values of $|V_{cb}|$ from $B \rightarrow D^{(*)}\ell\bar{\nu}$, which are both below the inclusive one, this is not feasible anymore.

In the exclusive case, the SM value of $|V_{cb}|$ relies on form factors (FFs), which can be obtained by different nonperturbative methods, in particular light-cone sum rules [11,20,21] and lattice QCD [22,23]. These FFs also enter the SM predictions for the ratios

$$\mathcal{R}(D^{(*)}) = \frac{\text{BR}(B \rightarrow D^{(*)}\tau\bar{\nu})}{\text{BR}(B \rightarrow D^{(*)}\ell\bar{\nu})}, \quad \ell = e, \mu, \quad (1)$$

testing lepton flavor universality (LFU). Here, a tension between the measurements of *BABAR* [24,25], *Belle* [26–30] and *LHCb* [31–34], whose average reads [12]

$$\begin{aligned} \mathcal{R}(D) &= 0.356 \pm 0.029, \\ \mathcal{R}(D^*) &= 0.284 \pm 0.013, \end{aligned} \quad (2)$$

and the SM prediction [12]²

$$\begin{aligned} \mathcal{R}_{\text{SM}}(D) &= 0.298 \pm 0.004, \\ \mathcal{R}_{\text{SM}}(D^*) &= 0.254 \pm 0.005, \end{aligned} \quad (3)$$

of 3.2σ exists. While in this case a new physics (NP) explanation is possible, and these ratios have the advantage of being fairly insensitive to hadronic uncertainties, the HFLAV value is challenged by alternative calculations of the FFs, in particular the one based on the dispersive matrix (DM) approach [35,36]. The DM FFs do not only reduce the tension in $\mathcal{R}(D^*)$ to 1.3σ [37], but also give $|V_{cb}| = (41.2 \pm 0.8) \times 10^{-3}$ from $B_{(s)} \rightarrow D_{(s)}^{(*)}\ell\nu$ [8,37,38], which agrees with the inclusive values of $(42.16 \pm 0.51) \times 10^{-3}$ [39] or $(41.69 \pm 0.63) \times 10^{-3}$ [40].

However, this agreement comes at the cost of creating tensions between the DM FFs and the ones measured in differential $B \rightarrow D^{(*)}\ell\nu$ distributions. While this opens up the possibility of NP coupling to light leptons (instead or in addition to taus) it is not clear that this is a feasible option once all experimental information is taken into account. Indeed, the *Belle* and *Belle II* collaborations recently released the results of the first measurement of the D^* longitudinal polarization fraction F_L^ℓ [41,42] finding

$$\begin{aligned} F_{L,\text{Belle}}^e &= 0.485 \pm 0.017 \pm 0.005, \\ F_{L,\text{Belle}}^\mu &= 0.518 \pm 0.017 \pm 0.005, \\ F_{L,\text{Belle II}}^e &= 0.521 \pm 0.005 \pm 0.007, \\ F_{L,\text{Belle II}}^\mu &= 0.534 \pm 0.005 \pm 0.006. \end{aligned} \quad (4)$$

Here, the first uncertainties are statistical while the second ones are systematic. Moreover, also the forward-backward asymmetry A_{FB}^ℓ was measured, for which they find

$$\begin{aligned} A_{\text{FB,Belle}}^e &= 0.230 \pm 0.018 \pm 0.005, \\ A_{\text{FB,Belle}}^\mu &= 0.252 \pm 0.019 \pm 0.005, \\ A_{\text{FB,Belle II}}^e &= 0.219 \pm 0.011 \pm 0.020, \\ A_{\text{FB,Belle II}}^\mu &= 0.215 \pm 0.011 \pm 0.022. \end{aligned} \quad (5)$$

For the case of F_L , while a small tension is present among the two measurements in the electron channel, the muon ones are in good agreement. The situation is opposite for A_{FB} , with the two measurements in the electron channel in good agreement, while a small discrepancy is present in the muon one. Importantly, the theoretical predictions for these quantities crucially depend on the choice of FF parametrization.

Given this new level of accuracy in these observables, it is imperative to inspect the impact of these measurements on the global $b \rightarrow c\ell\nu$ fit, including the dependence on the FF set used. In this article, we focus in particular on the DM FFs, compared to the FFs of Refs. [5,6,18,22]. For this, we first review the formalism used to describe $B \rightarrow D^*\ell\nu$ decays in Sec. II and give a short summary to the DM approach in Sec. III. Implications of the measurements of $F_L^{e,\mu}$ are discussed in Sec. IV before we conclude in Sec. V.

II. FORMALISM

The effective Hamiltonian

$$\begin{aligned} \mathcal{H}_{\text{eff}} = 2\sqrt{2}G_F V_{cb}[(1 + g_{V_L}^\ell)O_{V_L}^\ell + g_{V_R}^\ell O_{V_R}^\ell \\ + g_{S_L}^\ell O_{S_L}^\ell + g_{S_R}^\ell O_{S_R}^\ell + g_T^\ell O_T^\ell] + \text{H.c.}, \end{aligned} \quad (6)$$

with the dimension-six operators

$$\begin{aligned} O_{V_L}^\ell &= (\bar{c}\gamma^\mu P_L b)(\bar{\ell}\gamma_\mu P_L \nu_\ell), \\ O_{V_R}^\ell &= (\bar{c}\gamma^\mu P_R b)(\bar{\ell}\gamma_\mu P_L \nu_\ell), \\ O_{S_L}^\ell &= (\bar{c}P_L b)(\bar{\ell}P_L \nu_\ell), \\ O_{S_R}^\ell &= (\bar{c}P_R b)(\bar{\ell}P_L \nu_\ell), \\ O_T^\ell &= (\bar{c}\sigma^{\mu\nu} P_L b)(\bar{\ell}\sigma_{\mu\nu} P_L \nu_\ell), \end{aligned} \quad (7)$$

describes $\bar{B} \rightarrow D^*\ell\nu$ transitions within the SM and heavy NP extensions. Here $\sigma_{\mu\nu} = \frac{i}{2}[\gamma_\mu, \gamma_\nu]$ and $P_{L,R} = (1 \mp \gamma_5)/2$, and we do not consider here the case of light right-handed neutrinos. Note that at the dimension-six level in the SMEFT, g_{V_R} is lepton flavor-universal, implying $g_{V_R}^e = g_{V_R}^\mu = g_{V_R}^\tau$.

For the SM operator, the $B \rightarrow D^*$ matrix element is described as

²The HFLAV value is based on Refs. [1–3,5,6,8].

$$\begin{aligned} & \langle D^*(p, \epsilon) | \bar{c} \gamma^\mu P_L b | \bar{B}(p_B) \rangle \\ &= -\frac{V(q^2)}{m_B + m_{D^*}} \epsilon_{\alpha\beta\gamma}^\mu \epsilon^{*\alpha} p^\beta q^\gamma + iA_0(q^2) \frac{m_{D^*}}{q^2} (\epsilon^* \cdot q) q^\mu \\ &\quad - \frac{iA_1(q^2)}{2(m_B - m_{D^*})} [(m_B^2 - m_{D^*}^2) \epsilon^{*\mu} - (\epsilon^* \cdot q)(p + p_B)^\mu] \\ &\quad - iA_3(q^2) \frac{m_{D^*}}{q^2} (\epsilon^* \cdot q) \left[\frac{q^2}{m_B^2 - m_{D^*}^2} (p + p_B)^\mu - q^\mu \right], \end{aligned} \quad (8)$$

with

$$2m_{D^*} A_3(q^2) = (m_B + m_{D^*}) A_1(q^2) - (m_B - m_{D^*}) A_2(q^2), \quad (9)$$

where $q = p_B - p$, such that q^2 is the invariant mass of the dilepton pair. The FFs can be decomposed as

$$\begin{aligned} V(q^2) &= \frac{m_B + m_{D^*}}{2} g(w), \\ A_1(q^2) &= \frac{f(w)}{m_B + m_{D^*}}, \\ A_2(q^2) &= \frac{1}{2} \frac{m_B + m_{D^*}}{(w^2 - 1)m_B m_{D^*}} \left[\left(w - \frac{m_{D^*}}{m_B} \right) f(w) - \frac{\mathcal{F}_1(w)}{m_B} \right], \\ A_0(q^2) &= \frac{1}{2} \frac{m_B + m_{D^*}}{\sqrt{m_B m_{D^*}}} P_1(w), \end{aligned} \quad (10)$$

in the Boyd-Grinstein-Lebed (BGL) formalism [43–45] with

$$w = \frac{m_B^2 + m_{D^*}^2 - q^2}{2m_B m_{D^*}}. \quad (11)$$

The FFs obey two kinematical constraints: at zero recoil ($w = 1$), where only two out of the three helicity amplitudes are independent when the D^* meson is at rest,

$$\mathcal{F}_1(1) = (m_B - m_{D^*}) f(1) \quad (12)$$

holds, while at maximum recoil, due to the cancellation of any apparent kinematical singularity in the Lorentz decomposition of Eq. (8), we have

$$P_1(w_{\max}) = \frac{\mathcal{F}_1(w_{\max})}{(1 + w_{\max})(m_B - m_{D^*}) \sqrt{m_B m_{D^*}}}. \quad (13)$$

Here, we introduced w_{\max} which for a massless lepton reads

$$w_{\max} = \frac{m_B^2 + m_{D^*}^2}{2m_B m_{D^*}} \simeq 1.504. \quad (14)$$

We can now define the differential decay width as

$$\begin{aligned} \frac{d\Gamma(B \rightarrow D^*(\rightarrow D\pi)\ell\nu)}{dw d\cos\theta_\ell d\cos\theta_D d\chi} &= \frac{G_F^2 |V_{cb}|^2}{4(4\pi)^4} 3m_B m_{D^*} \sqrt{w^2 - 1} \left(1 - 2 \frac{m_{D^*}}{m_B} w + \frac{m_{D^*}^2}{m_B^2} \right) B(D^* \rightarrow D\pi) \\ &\times \{ (1 - \cos\theta_\ell)^2 \sin^2\theta_D |H_+|^2 + (1 + \cos\theta_\ell)^2 \sin^2\theta_D |H_-|^2 + 4 \sin^2\theta_\ell \cos^2\theta_D |H_0|^2 \\ &- 2 \sin^2\theta_\ell \sin^2\theta_D \cos 2\chi H_+ H_- - 4 \sin\theta_\ell (1 - \cos\theta_\ell) \sin\theta_D \cos\theta_D \cos\chi H_+ H_0 \\ &+ 4 \sin\theta_\ell (1 + \cos\theta_\ell) \sin\theta_D \cos\theta_D \cos\chi H_- H_0 \}, \end{aligned} \quad (15)$$

in the massless lepton limit.³ In the differential width, the angle (in the virtual W boson rest frame) between the lepton and the direction opposite to the B meson momentum is defined as θ_ℓ ; the angle in the D^* rest frame between the D meson and the direction opposite the B meson momentum is θ_D , and finally the angle in the B meson rest frame between the two decay planes spanned by the $D^* - D$ and $W - \ell$ systems is χ .

In Eq. (15) we have introduced the helicity amplitudes

$$\begin{aligned} H_0(w) &= \frac{\mathcal{F}_1(w)}{\sqrt{m_B^2 + m_{D^*}^2 - 2m_B m_{D^*} w}}, \\ H_\pm(w) &= f(w) \mp m_B m_{D^*} \sqrt{w^2 - 1} g(w), \end{aligned} \quad (16)$$

³In our analysis we nevertheless keep the full lepton mass dependence which introduces the additional FF P_1 .

which enter in the decay rate, in the D^* longitudinal polarization fraction and in the forward-backward asymmetry:

$$\frac{d\Gamma}{dw} \propto |H_0(w)|^2 + |H_+(w)|^2 + |H_-(w)|^2, \quad (17)$$

$$F_L^\ell(w) = \frac{|H_0(w)|^2}{|H_0(w)|^2 + |H_+(w)|^2 + |H_-(w)|^2}, \quad (18)$$

$$A_{FB}^\ell(w) = \frac{|H_-(w)|^2 - |H_+(w)|^2}{|H_0(w)|^2 + |H_+(w)|^2 + |H_-(w)|^2}. \quad (19)$$

These quantities are usually predicted and measured after integrating the helicity amplitudes over the available phase space, i.e., $w \in [1, w_{\max}]$. This implies an interesting feature for the $\mathcal{F}_1(w)$ FF: if its integral over the phase space

increases, e.g., due to an increase of $\mathcal{F}_1(w)$ at large w , this induces an increase for both observables in Eqs. (17)–(18) and a decrease for the one in Eq. (19). Remembering now the definition of $\mathcal{R}(D^*)$ in Eq. (1), we observe that an increase in the light lepton $d\Gamma/dw$ induces a decrease in the LFUV ratio. We can therefore infer that a change of the shape of $\mathcal{F}_1(w)$, resulting in an increase (decrease) of its integrated value, would imply an increase (decrease) for the prediction for F_L^ℓ and a decrease (increase) for the ones of $\mathcal{R}(D^*)$ and A_{FB}^ℓ . As we will see in Sec. IV, this is crucial for understanding how the DM FFs affect the predictions for F_L^ℓ and A_{FB}^ℓ within the SM.

III. SUMMARY OF FORM FACTORS

- We give a short description of the four FF sets we use.⁴
- (i) DM: See detailed explanation below;
 - (ii) F/M: The results obtained employing the lattice QCD by the Fermilab(FNAL)/MILC collaboration [22], which for the first time computed the FFs at nonzero recoil and analyzed them with the BGL parametrization, which is model-independent and based only on QCD dispersion relations⁵;
 - (iii) BGJS: The recent results by Bigi, Gambino, Jung, and Schacht [5,49,50] without the inclusion of FNAL/MILC data [22] obtained employing the BGL parametrization [45] at the (2,2,2) truncation order; the additional pseudoscalar FF P_1 entering in $R(D^*)$ is extracted rescaling the FF A_1 by an appropriate ratio, computed in HQET [2], and making use of the constraint (13), which applies at maximum recoil⁶;
 - (iv) IgWa: An approach developed in Refs. [6,17] to go beyond the original formulation of HQET [47,48], that adopts a systematic expansion in terms of

⁴We do not include the CLN parametrization [46], obtained by applying heavy quark symmetry to FFs based on the heavy quark effective theory (HQET) [47,48] due to several issues: first, an inconsistent treatment of FF ratios when going beyond zero recoil in its experimental implementations (which was however not originally present in Ref. [46]) led to inconsistent results already at first order in HQET [2]; moreover, the constraint between the slope and curvature of the leading Isgur-Wise function are problematic; finally, this method uses approximations such that it is, e.g., not possible to consistently incorporate Λ_{QCD}^2/m_c^2 correction which are non-negligible [17].

⁵Novel results have recently been released by the HPQCD collaboration as well [23], compatible at the 1σ level with the FNAL/MILC results. We do, however, not consider this set in our analysis, because, on the one hand, it is not published yet, and, on the other hand, the DM results are based on the FNAL/MILC results only, which are therefore the natural lattice results to compare with.

⁶A modified BGL expansion, which is characterized by a built-in unitarity condition, has recently been proposed in Ref. [51]. However, we do not use it in this work since the results of its direct application to semileptonic $B \rightarrow D^*$ decays are not available at present.

inverse powers of heavy quark masses and in particular incorporates Λ_{QCD}^2/m_c^2 corrections coming from heavy quark symmetry considerations [52]; in our numerical study we employ the latest results by Iguro and Watanabe based on their (2/1/0) truncation order [18]; we stress that these method employs as external input information coming from light-cone sum rules [21] and QCD sum rules [53–55] as well, in order to constrain its parameters.

Let us now consider the DM formalism in some more detail, as these FFs have never been used before in a global fit. The DM approach is a nonperturbative method for computing hadronic FFs in a model-independent way [35], applied, in particular, to the investigation of $B \rightarrow D^{(*)}\ell\nu_\ell$ [8,37], $B_s \rightarrow D_s^{(*)}\ell\nu_\ell$ [38] and $B(B_s) \rightarrow \pi(K)\ell\nu_\ell$ [56] decays.

The starting point is a dispersion relation that, for a generic FF f can be written as [45,46,57]

$$\frac{1}{2\pi i} \oint_{|z|=1} \frac{dz}{z} |\phi(z)f(z)|^2 \leq \chi, \quad (20)$$

where $\phi(z)$ is a function depending on the specific spin-parity channel (and including the Blaschke factors needed to remove subthreshold bound-state poles) and χ is the so-called susceptibility related to the derivative of the Fourier transform of a suitable Green function of bilinear quark operators [45], calculated within lattice QCD in Ref. [36] for several spin-parity channels of interest. The conformal variable $z(t)$ is defined as

$$z(t) = \frac{\sqrt{t_+ - t} - \sqrt{t_+ - t_-}}{\sqrt{t_+ - t} + \sqrt{t_+ - t_-}}, \quad (21)$$

with $t = q^2$ being the squared 4-momentum transfer and $t_\pm \equiv (m_B \pm m_{D^*})^2$ for the case of interest in this work. By introducing the inner product [58,59]

$$\langle g | h \rangle = \frac{1}{2\pi i} \oint_{|z|=1} \frac{dz}{z} \bar{g}(z)h(z), \quad (22)$$

where $\bar{g}(z)$ is the complex conjugate of the function $g(z)$, Eq. (20) can be also written as

$$0 \leq \langle \phi f | \phi f \rangle \leq \chi. \quad (23)$$

Following Refs. [58,59] we introduce the set of functions

$$g_t(z) \equiv \frac{1}{1 - \bar{z}(t)z}, \quad (24)$$

where $\bar{z}(t)$ is the complex conjugate of the conformal variable $z(t)$, so that the use of Cauchy's theorem yields

$$\langle g_t | \phi f \rangle = \phi(z(t))f(z(t)), \quad (25)$$

$$\langle g_{t_m} | g_{t_l} \rangle = \frac{1}{1 - \bar{z}(t_l) z(t_m)}. \quad (26)$$

The central ingredient of the DM method is the matrix [58,59]

$$\mathbf{M} \equiv \begin{pmatrix} \langle \phi f | \phi f \rangle & \langle \phi f | g_t \rangle & \langle \phi f | g_{t_1} \rangle & \cdots & \langle \phi f | g_{t_N} \rangle \\ \langle g_t | \phi f \rangle & \langle g_t | g_t \rangle & \langle g_t | g_{t_1} \rangle & \cdots & \langle g_t | g_{t_N} \rangle \\ \langle g_{t_1} | \phi f \rangle & \langle g_{t_1} | g_t \rangle & \langle g_{t_1} | g_{t_1} \rangle & \cdots & \langle g_{t_1} | g_{t_N} \rangle \\ \vdots & \vdots & \vdots & \vdots & \vdots \\ \langle g_{t_N} | \phi f \rangle & \langle g_{t_N} | g_t \rangle & \langle g_{t_N} | g_{t_1} \rangle & \cdots & \langle g_{t_N} | g_{t_N} \rangle \end{pmatrix}, \quad (27)$$

where t_1, \dots, t_N are the values of the squared 4-momentum transfer at which the FF $f(z)$ is known. In the DM method we consider only values $f(z(t_i))$ (with $i = 1, 2, \dots, N$) computed nonperturbatively on the lattice.

The important feature of the matrix \mathbf{M} is that, thanks to the positivity of the inner products, its determinant is positive semidefinite, i.e., $\det \mathbf{M} \geq 0$. This property is not modified when the first matrix element in Eq. (27) is replaced by the upper bound given by the susceptibility χ through Eq. (23). Thus, using also the fact that both z and $f(z)$ can assume only real values in the allowed kinematical region for semileptonic decays, the original matrix (27) can be replaced by

$$\mathbf{M}_\chi = \begin{pmatrix} \chi & \phi f & \phi_1 f_1 & \cdots & \phi_N f_N \\ \phi f & \frac{1}{1-z^2} & \frac{1}{1-z z_1} & \cdots & \frac{1}{1-z z_N} \\ \phi_1 f_1 & \frac{1}{1-z_1 z} & \frac{1}{1-z_1^2} & \cdots & \frac{1}{1-z_1 z_N} \\ \cdots & \cdots & \cdots & \cdots & \cdots \\ \phi_N f_N & \frac{1}{1-z_N z} & \frac{1}{1-z_N z_1} & \cdots & \frac{1}{1-z_N^2} \end{pmatrix}, \quad (28)$$

where $\phi_i f_i \equiv \phi(z_i) f(z_i)$ (with $i = 1, 2, \dots, N$) represent the known values of $\phi(z) f(z)$ corresponding to the given set of values z_i .

By imposing the positivity of the determinant of the matrix (28) it is possible to explicitly compute the lower and upper bounds that unitarity imposes on the FF $f(z)$ for a generic value of z , namely [35]

$$\beta(z) - \sqrt{\gamma(z)} \leq f(z) \leq \beta(z) + \sqrt{\gamma(z)}, \quad (29)$$

where

$$\beta(z) \equiv \frac{1}{\phi(z) d(z)} \sum_{j=1}^N \phi_j f_j d_j \frac{1-z_j^2}{z-z_j}, \quad (30)$$

$$\gamma(z) \equiv \frac{1}{1-z^2} \frac{1}{\phi^2(z) d^2(z)} (\chi - \chi_{\text{DM}}), \quad (31)$$

$$\chi_{\text{DM}} \equiv \sum_{i,j=1}^N \phi_i f_i \phi_j f_j d_i d_j \frac{(1-z_i^2)(1-z_j^2)}{1-z_i z_j}, \quad (32)$$

$$d(z) \equiv \prod_{m=1}^N \frac{1-z z_m}{z-z_m}, \quad (33)$$

$$d_j \equiv \prod_{m \neq j=1}^N \frac{1-z_j z_m}{z_j-z_m}. \quad (34)$$

Unitarity is satisfied only when $\gamma(z) \geq 0$, which implies $\chi \geq \chi_{\text{DM}}$ and represents a parametrization-independent test of it for a given set of input values f_j . In this way, the input data are filtered by unitarity. Within the DM approach only the subset of input data satisfying the unitary filter $\chi \geq \chi_{\text{DM}}$ is considered.

Moreover, when $z \rightarrow z_j$ one has $\beta(z) \rightarrow f_j$ and $\gamma(z) \rightarrow 0$ (see Ref. [35]). In other words, Eq. (29) exactly reproduces the input unitary data, i.e., the subset satisfying the unitary filter $\chi \geq \chi_{\text{DM}}$. Therefore, the DM band for the form factor $f(z)$ at a generic value of z is given by the convolution of the uniform distribution corresponding to Eqs. (30)–(31) with the distribution of the input (lattice) data $\{f_j\}$ having $\chi \geq \chi_{\text{DM}}$. It represents the envelope of the results of all possible (either truncated or not truncated) z -expansions, like the BGL one [45], which satisfy unitarity and at the same time exactly reproduce the input unitary data. In a frequentist language, this corresponds to a null value of the χ^2 -variable. This is at variance with what happens when working directly with (either truncated or not truncated) BGL fits, which may have $\chi^2 > 0$ even when the fitting function is constructed to satisfy unitarity.

For the purpose of our numerical analysis, for each of ten equally spaced recoil bins of the $B \rightarrow D^*$ channel we use a linear parametrization of the four DM FFs of the form

$$f_i(w) = a_i + w \cdot b_i. \quad (35)$$

We stress that this is in not an expansion of the FFs in w , but rather a simple interpolation, bin by bin, of the full bands obtained in Ref. [37]. The values of the parameters a_i and b_i , their associated errors and their correlations (which we report in Appendix) are fixed by the reproduction of the values of the DM form factor $f_i(w)$ at the boundaries of the i th experimental bin. Indeed, we have checked that with such a parametrization, the predicted values for $\mathcal{R}(D^*)$ and F_L^r [37] are accurately reproduced. We then use values for each a_i and b_i , assuming normally distributed errors and including correlations among the total of 80 values. The same procedure is adopted for the two FFs describing the $B \rightarrow D$ channel.

IV. IMPACT OF F_L^ℓ AND A_{FB}^ℓ

A. SM predictions and fit

In our analysis we distinguish between *predictions* and *fits*. In the former case, we only use the theoretical results

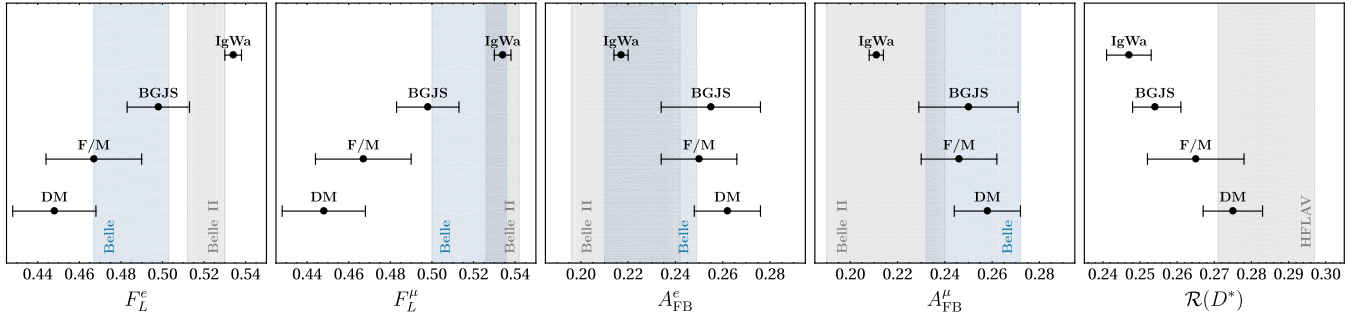


FIG. 1. Comparisons among measurements [12,41,42] and SM predictions for F_L^ℓ , A_{FB}^ℓ and $\mathcal{R}(D^*)$ at the 1σ level. See Sec. IV A for details on the different predictions.

relevant to each approach as priors in our analyses, without employing any further (experimental) information; in the latter case, all the relevant experimental results, like, e.g., Refs. [41,42], are enforced in the likelihood as well.

Let us start by studying F_L^ℓ and A_{FB}^ℓ in the SM within the four sets of FFs discussed in the previous section. In the absence of NP, and without using any additional experimental information, F_L^ℓ ($\ell = e, \mu$) is predicted to be

$$\begin{aligned} F_{L,DM}^\ell &= 0.448 \pm 0.020, \\ F_{L,F/M}^\ell &= 0.467 \pm 0.023, \\ F_{L,BGJS}^\ell &= 0.498 \pm 0.015, \\ F_{L,IgWa}^\ell &= 0.534 \pm 0.002, \end{aligned} \quad (36)$$

which has to be compared with Eq. (4). Similarly, the predictions for $A_{FB}^{e,\mu}$ read

$$\begin{aligned} A_{FB,DM}^{e(\mu)} &= 0.262(0.258) \pm 0.014, \\ A_{FB,F/M}^{e(\mu)} &= 0.250(0.246) \pm 0.016 \\ A_{FB,BGJS}^{e(\mu)} &= 0.255(0.250) \pm 0.021, \\ A_{FB,IgWa}^{e(\mu)} &= 0.217(0.211) \pm 0.003, \end{aligned} \quad (37)$$

to be compared with Eq. (5). A visual summary can be found in Fig. 1. Note that at the current level of precision, there is no difference among the predictions of F_L^e and F_L^μ , while A_{FB}^e and A_{FB}^μ slightly differ.

For F_L^ℓ we observe in the DM approach compatibility in the electron channel with the Belle result but a $\sim 2.5\sigma$ tension with Belle II. In the muon channel, the tension is even $\sim 2\sigma$ ($\sim 3\sigma$) compared to the Belle (II) result. In the FNAL/MILC and BGJS approaches the tension is smaller, while the IgWa FFs describe data very well. Concerning A_{FB}^ℓ , the DM approach predicts values slightly above both Belle II measurements, while well reproducing the Belle ones. On the other hand, the IgWa FFs have a prediction lower than the Belle muon measurement but describe well the other data. Finally, both FNAL/MILC and BJSL results are in good agreement with all measured values.

To better understand these differences in the predictions of F_L^ℓ and A_{FB}^ℓ , it is useful to study their q^2 behavior, as shown in the two panels of Fig. 2. The deviation between the DM and FNAL/MILC predictions originate from deviations in the shapes at smaller q^2 . This behavior is expected since the DM FFs use lattice input at low recoil, and a deviation among the two methods at large recoil can be traced back to the kinematic constraint in Eq. (13),

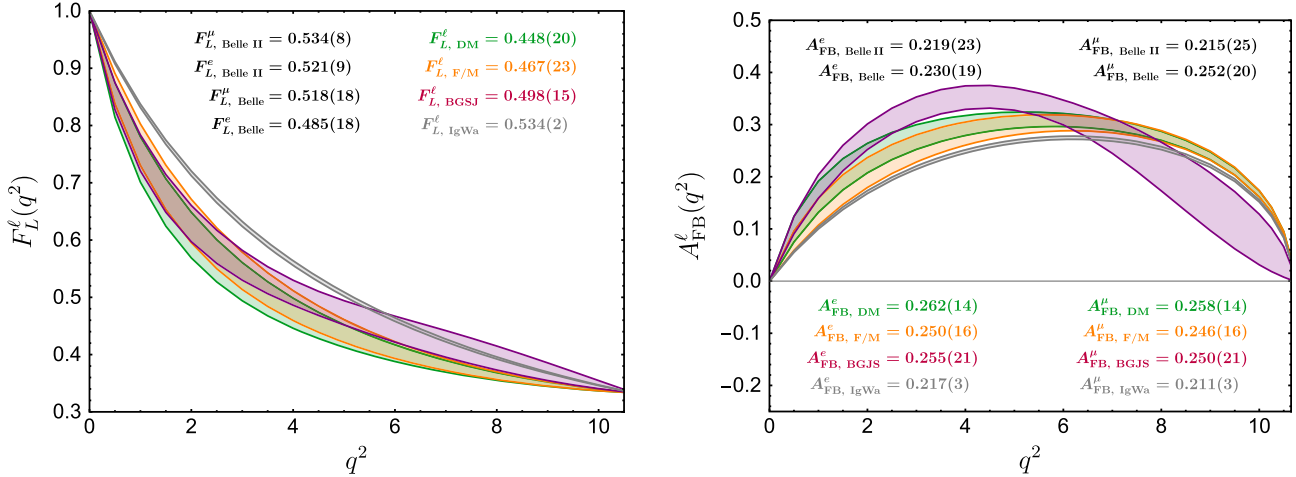


FIG. 2. Predicted 1σ range for F_L^ℓ (left panel) and A_{FB}^ℓ (right panel) as a function of q^2 for the four different FF sets.

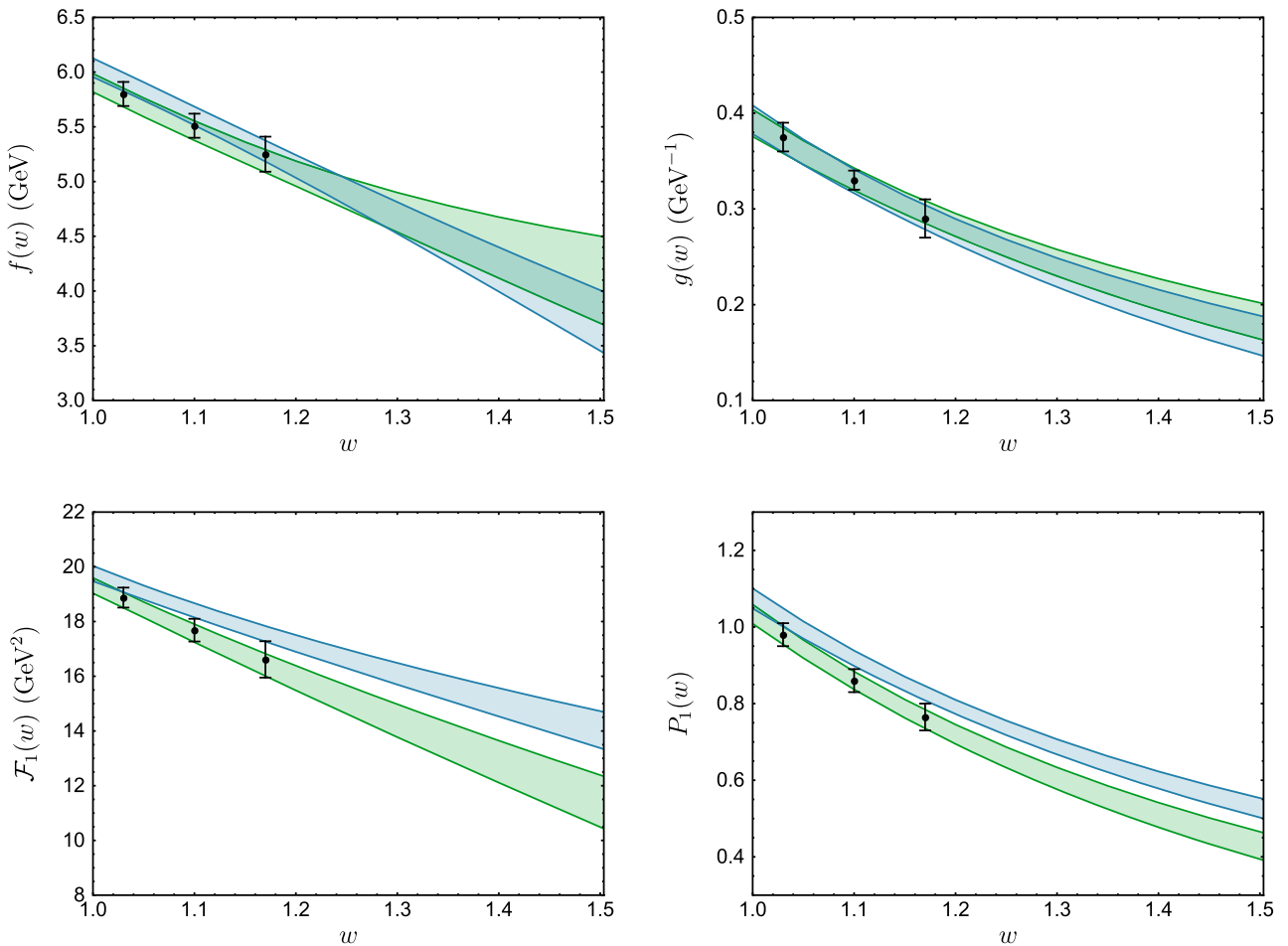


FIG. 3. $f(w)$ (top left panel), $g(w)$ (top right panel), $\mathcal{F}_1(w)$ (bottom left panel) and $P_1(w)$ (bottom right panel) in the DM approach when performing a prediction (green band) or a global fit (blue band); the black points and error bars denote the FNAL/MILC results [22], which are used to calculate the green band. See Sec. IV A for a discussion.

enforced only for the DM FFs. The values predicted in the BGJS approach deviate from the ones of the previous methods due to a difference in the shapes of the two observables. On the other hand, the IgWa results share the same shape with DM and FNAL/MILC while being shifted toward larger (lower) values for F_L^ℓ (A_{FB}^ℓ), and display the smallest overall uncertainty.

Let us now focus on the DM FFs, which predict $\mathcal{R}(D^*)$ to be in agreement with the measurements while having significant tensions in F_L^ℓ and, to a lesser extent, in A_{FB}^ℓ . We perform a fit with HEPfit [60] in which we include the τ lepton polarization $P_\tau(D^*)$ [61], the longitudinal polarization fraction in τ decays F_L^τ [62], $\mathcal{R}(D^{(*)})$ [12] and the longitudinal polarization fractions for light leptons F_L^ℓ and forward-backward asymmetries A_{FB}^ℓ [41,42].⁷ The parameters we vary in the fit are the 80 a_i and b_i correlated FF parameters, for which we assume a multivariate gaussian

⁷We refrain from including the differential results of Refs. [63,64] in our fit, given the potential incompatibility among the two results, see, e.g., Ref. [5].

prior, and whose central values, errors and correlations are reported in Appendix. We obtain the following results for all the relevant observables currently measured:

$$\begin{aligned} \mathcal{R}(D^*)_{\text{fit}} &= 0.265 \pm 0.005, \\ F_{L,\text{fit}}^\ell &= 0.515 \pm 0.005, \\ A_{FB,\text{fit}}^\ell &= 0.227 \pm 0.007, \\ A_{FB,\text{fit}}^\mu &= 0.222 \pm 0.007. \end{aligned} \quad (38)$$

This means that the pull of the F_L^ℓ and A_{FB}^ℓ measurements on the shape of the FFs (for which, we remind, the SM values of the DM FFs act only as priors) are so strong that the postfit values of the polarization fractions and asymmetries are compatible with data at the 1σ level, while a small tension at 1.5σ level in $\mathcal{R}(D^*)$ reemerges. We, therefore, find ourselves in a situation similar to the other FF sets, i.e., agreement within F_L^ℓ and A_{FB}^ℓ but tension in $\mathcal{R}(D^*)$ (even though the latter is a bit less severe).

In order to understand how the predicted values for F_L^ℓ and A_{FB}^ℓ in Eqs. (36)–(37) are related to the postfit ones

given in Eq. (38), it is useful to study the shape of the FFs in the two scenarios. We report them in Fig. 3, together with the lattice data points [22] used in the DM approach. One sees that while the shape of $f(w)$ and $g(w)$ are not particularly altered when performing a global fit, the FFs $\mathcal{F}_1(w)$ and $P_1(w)$ show a $\sim 30\%$ growth at $w \simeq 1.5$.⁸ Moreover, the shape of $\mathcal{F}_1(w)$ and $P_1(w)$ are stretched to a point hardly compatible with the original DM values (prefit), not only at high recoil but also for lower values of w , where they now fail to reproduce lattice data. Hence, not only the tensions with data are present as in all other FF approaches, but in addition the postfit FF shapes disagree with the lattice data used as input. Note that a similar tension among the experimental differential decay widths of Refs. [63,64] and the theoretical lattice data of Ref. [22] has already been pointed out in Refs. [22,37].

Given this change in the FF shapes, it is interesting to study the implications regarding the extraction of $|V_{cb}|$. Going through the details of a systematic analysis of the correlated differential distributions from Refs. [63,64] is beyond the scope of this paper; however, as originally proposed in Ref. [65], the CKM matrix element $|V_{cb}|$ can also be extracted from a comparison among the experimental determination of the total branching ratio and the corresponding theoretical value (modulo $|V_{cb}|^2$). The values of the total experimental branching ratio here considered are $\mathcal{B}(B \rightarrow D^* \ell \bar{\nu}) = (4.95 \pm 0.11 \pm 0.22) \times 10^{-2}$ [63] and $\mathcal{B}(B \rightarrow D^* \ell \bar{\nu}) = (5.04 \pm 0.02 \pm 0.16) \times 10^{-2}$ [64]. Following this procedure, the final value extracted for $|V_{cb}|$ corresponding to the FFs described by the green bands in Fig. 3 equals to $|V_{cb}| = (43.1 \pm 1.2) \times 10^{-3}$, while the one induced by the FFs described by the blue bands in the same figure equals to $|V_{cb}|_{\text{fit}} = (41.2 \pm 1.2) \times 10^{-3}$, which is compatible with the inclusive determinations. It is also compatible with the value predicted by a unitarity triangle analysis (UTA), equal to $|V_{cb}| = (42.22 \pm 0.51) \times 10^{-3}$ [14,15] and obtained considering in the global analysis all relevant channels except the ones directly contributing to $|V_{cb}|$.⁹ Let us finally highlight that systematic experimental uncertainties due to a proper estimation of the backgrounds and to the application of kinematical cuts (concerning in particular the lepton momentum) may arise at the percent

⁸The changes in $\mathcal{F}_1(w)$ shape (and therefore in $P_1(w)$ one) is expected from Eq. (38), since an increase of its integrated value induces an enhancement of F_L^ℓ and a decrease of A_{FB}^ℓ and $\mathcal{R}(D^*)$, as detailed at the end of Sec. II.

⁹The slopes of the FFs corresponding to the green bands in Fig. 3 do not agree with the experimental differential distributions by Belle [63,64], as clearly visible from Fig. 3 of Ref. [37]. This *slope tension* is the reason of the FNAL/MILC result for $|V_{cb}|$, namely $|V_{cb}| = (38.4 \pm 0.8) \times 10^{-3}$, as given in Ref. [22]. The difference with respect to our quoted value $|V_{cb}| = (43.1 \pm 1.2) \times 10^{-3}$ is due to the fact that our procedure, instead, involves only integrals of the form factors over the total experimental decay range. In this sense, it is complementary to the one that can be obtained through a study of the experimental differential data.

level. These effects will have to be taken carefully into account especially in future analyses, namely when the precision on the theoretical computations of the FFs will importantly increase.

B. NP involving light leptons

While it is well known that a deviation in $\mathcal{R}(D^*)$ can be explained by NP effects related to taus (see, e.g., Refs. [66,67] for very early accounts), it is interesting to see whether the predictions for F_L^ℓ and A_{FB}^ℓ with the DM FFs can be addressed by NP coupled to light leptons [68,69]. In the following, due to the strong constraint from $\mathcal{R}_{e\mu}^{D^*} = \text{BR}(B \rightarrow D^* e \bar{\nu}) / \text{BR}(B \rightarrow D^* \mu \bar{\nu}) = 0.990 \pm 0.031$ [41] and $\mathcal{R}_{e\mu}^{D^*} = 1.001 \pm 0.023$ [42], we assume LFU contributions to electrons and muons, namely $g_i^\ell = g_i^\mu \equiv g_i$.¹⁰

Since left-handed vector operators only change the total decay width, we consider scalar and tensor operators as well as the right-handed vector current.¹¹ However, when considering NP effects to one operator at a time, no significant preference for any nonvanishing Wilson coefficient is found.¹² The bounds at the 1σ level read

$$\begin{aligned} g_{V_R} &\in [-0.04, 0.01], \\ g_{S_L} &\in [-0.07, 0.02], \\ g_{S_R} &\in [-0.05, 0.03], \\ g_T &\in [-0.01, 0.02]. \end{aligned} \quad (39)$$

These results are not significantly changed if all coefficients are considered at the same time in a four-dimensional fit. This means that the tension between the F_L^ℓ measurements and the prediction using the DM FFs cannot be explained by NP as F_L^ℓ is very insensitive to it. This is in contrast to the case of NP coupled to tau leptons, where hints for scalar and/or tensor operators can be found, and F_L^τ and A_{FB}^τ can be significantly altered by their presence (see, e.g., Refs. [68,70,71] for recent reviews). This feature can be ascribed to the more accurate measurements for light lepton channels and the m_ℓ suppression in interference terms of scalar or tensor operators with the SM contribution.

If F_L^ℓ is included in the fit, a tension in $\mathcal{R}(D^*)$ reemerges, but is still smaller than for the other FF sets. Therefore, it could be possible to explain these tensions with the SM operator $O_{V_L}^\ell$ related to light leptons (while for the other FF sets, a full explanation requires NP in taus). Performing a global fit in this setup to g_{V_L} with light leptons, we obtain

¹⁰We have checked that allowing for different NP effects in electrons and muons does not change the picture.

¹¹As explained in Sec. II, we assume LFU contributions in all three leptons for the case of g_{V_R} .

¹²Including NP effects in the scalar or tensor currents induces the presence of three additional matrix elements in the amplitude. In order to include the corresponding FFs, we rely on the results obtained in Ref. [2].

$$\begin{aligned}
\mathcal{R}(D)_{g_{V_L}} &= 0.335 \pm 0.009, \\
\mathcal{R}(D^*)_{g_{V_L}} &= 0.291 \pm 0.009, \\
F_{L,g_{V_L}}^\ell &= 0.515 \pm 0.005, \\
A_{FB,g_{V_L}}^e &= 0.227 \pm 0.007, \\
A_{FB,g_{V_L}}^\mu &= 0.222 \pm 0.007,
\end{aligned} \tag{40}$$

corresponding to $g_{V_L} = -0.054 \pm 0.015$. As expected, g_{V_L} induces only an overall normalization factor, and therefore both the longitudinal polarization fraction and the forward-backward asymmetry are insensitive to it, i.e., their values stay unchanged compared to Eq. (38). Hence, the tensions in $\mathcal{F}_1(w)$ and $P_1(w)$ between their predictions within DM and the fitted values are still present.

The presence of NP in $O_{V_L}^\ell$ alters the extraction of $|V_{cb}|$ by a factor of $1/(1 + g_{V_L})$. According to our fit results, $|V_{cb}|_{\text{fit}} = (41.2 \pm 1.2) \times 10^{-3}$ from $B \rightarrow D^* \ell \nu$ would be shifted to $|V_{cb}|_{g_{V_L}} = (43.6 \pm 1.4) \times 10^{-3}$. This value is still compatible with the inclusive one, which receives the same correction $1/(1 + g_{V_L})$, and is not too large to spoil other indirect measurements like $\Delta F = 2$ processes, sensitive to NP contributions. Finally, note that g_{V_L} is small enough to evade constraints from high- p_T lepton tail searches [72] which require $|g_{V_L}| < 0.25$ [73].

Importantly, an explanation via NP related to light leptons is only possible when employing the DM FFs in a global fit, albeit their significant deformation with respect to their original shape. As stated above, such deformations points to a tension of lattice predictions with experiment, as also seen in the differential decay widths. On the other hand, the other FF approaches, due to the larger discrepancy in $\mathcal{R}(D^*)$, require larger values for g_{V_L} which, if related to light leptons, would induce a shift in $|V_{cb}|$ too large to be compatible with the UTA and high- p_T constraints [74,75].

V. CONCLUSIONS

The SM predictions for $B \rightarrow D^* \ell \nu$ decays depend critically on the FFs used to calculate them. While most sets of FFs lead to significant tensions with the measurements of $\mathcal{R}(D^*)$, the DM approach results in a SM value compatible with experiment. In order to further assess the agreement of the different FF sets with data, we investigated the impact of the recent measurements of the longitudinal D^* polarization fraction F_L^ℓ for $\ell = e, \mu$ by Belle [41] and Belle II [42], as well as that of A_{FB}^ℓ . While FNAL/MILC, IgWa and BGJS lead to SM values in agreement with the experimental results, the DM predictions show significant tensions with them, up to the $\sim 3\sigma$ level.

While it is well known that $\mathcal{R}(D^*)$ can be accounted for by physics beyond the SM, we find that NP cannot explain the tension in F_L^ℓ . The reason for this is that F_L^ℓ (with light

leptons) is very insensitive to NP contributions, such that the constraints from other observables prevent a consistent NP explanation within a global fit. We then included F_L^ℓ within a global fit within the DM approach, using the theory predictions for the parameters as priors, and found that the pull on these parameters is so strong that it violently deforms them. One then ends up in a situation similar to the other three FF sets with a significant (unaccounted) tension in $\mathcal{R}(D^*)$, which is however still smaller than in the other cases.

This decreased tension allows for an explanation via g_{V_L} with (only) light leptons (contrary to the other FFs where NP in tau leptons is needed), without causing problems in the determination of $|V_{cb}|$ or being in tension with direct LHC searches. However, a tension with the shape of the FFs predicted on the lattice is unavoidable, similar to the one observed previously [22,37] when comparing lattice results [22] to experimental differential decay widths [63,64].

ACKNOWLEDGMENTS

The authors wish to thank Guido Martinelli and Manuel Naviglio for useful discussions, and Markus Prim and Chaoyi Lyu for fruitful exchanges about the recent Belle and Belle II results. The work of M. B., M. F., S. I. and U. N. is supported by the Deutsche Forschungsgemeinschaft (DFG, German Research Foundation) under Grant No. 396021762-TRR 257. A. C. is supported by a Professorship Grant (PP00P2_176884) of the Swiss National Science Foundation. S. S. is supported by the Italian Ministry of University and Research (MIUR) under Grant No. PRIN20172LNEEZ. The work of L. V. is supported by ANR under Contract No. 202650 (ANR-19-CE31-0016, GammaRare). U. N. acknowledges the hospitality of Fermilab and thanks Jim Simone and Andreas Kronfeld for helpful discussions.

APPENDIX: DM PARAMETERS AND CORRELATIONS

In this Appendix, we provide to the reader the information necessary in order to reproduce the DM analyses performed in our study. As detailed in Sec. III, each FF is linearly parameterized by the form $f_i(w) = a_i + w \cdot b_i$, employing different values for the parameters a_i and b_i in ten recoil bins. In particular, the boundaries of the ten w bins are

$$\begin{aligned}
&\{1.00, 1.05, 1.10, 1.15, 1.20, 1.25, 1.30, 1.35, \\
&1.40, 1.45, 1.504\}.
\end{aligned} \tag{A1}$$

The numerical values and the associated errors of the a_i parameters for the four FFs in the ten w bins are given in Table I, while the values relative to the b_i parameters are provided in Table II. Correlations among all the parameters are listed in Tables III–XXXVIII.

TABLE I. Numerical values and their associated errors for the a_i parameters employed in our analyses.

Bin	a_f	a_g	$a_{\mathcal{F}_1}$	a_{P_1}
1	10.18(0.61)	1.019(0.087)	37.5(2.4)	2.88(0.16)
2	9.95(0.59)	0.953(0.078)	37.1(2.3)	2.68(0.14)
3	9.72(0.63)	0.893(0.070)	36.6(2.3)	2.50(0.13)
4	9.49(0.70)	0.837(0.064)	36.2(2.5)	2.34(0.12)
5	9.28(0.78)	0.786(0.059)	35.9(2.6)	2.19(0.11)
6	9.08(0.87)	0.739(0.054)	35.5(2.8)	2.05(0.10)
7	8.88(0.95)	0.696(0.051)	35.1(3.0)	1.92(0.09)
8	8.69(1.03)	0.656(0.048)	34.8(3.2)	1.80(0.08)
9	8.50(1.10)	0.619(0.045)	34.5(3.5)	1.69(0.08)
10	8.32(1.16)	0.584(0.043)	34.2(3.8)	1.59(0.07)

TABLE II. Numerical values and their associated errors for the b_i parameters employed in our analyses.

Bin	b_f	b_g	$b_{\mathcal{F}_1}$	b_{P_1}
1	-4.26(0.58)	-0.628(0.078)	-18.2(2.3)	-1.85(0.15)
2	-4.04(0.55)	-0.565(0.069)	-17.7(2.2)	-1.66(0.13)
3	-3.83(0.57)	-0.510(0.062)	-17.4(2.3)	-1.50(0.12)
4	-3.64(0.63)	-0.462(0.056)	-17.0(2.4)	-1.36(0.11)
5	-3.46(0.69)	-0.420(0.052)	-16.7(2.5)	-1.23(0.10)
6	-3.29(0.76)	-0.382(0.048)	-16.4(2.7)	-1.12(0.09)
7	-3.14(0.81)	-0.349(0.045)	-16.1(2.8)	-1.02(0.08)
8	-3.00(0.87)	-0.319(0.043)	-15.9(2.9)	-0.93(0.08)
9	-2.87(0.91)	-0.293(0.040)	-15.6(3.1)	-0.85(0.07)
10	-2.75(0.96)	-0.269(0.039)	-15.5(3.2)	-0.78(0.07)

TABLE III. Correlations among the a_f and a_f parameters.

	a_f^1	a_f^2	a_f^3	a_f^4	a_f^5	a_f^6	a_f^7	a_f^8	a_f^9	a_f^{10}
a_f^1	1.0	0.94	0.79	0.64	0.51	0.41	0.33	0.27	0.23	0.19
a_f^2	0.94	1.0	0.95	0.87	0.78	0.7	0.64	0.59	0.55	0.51
a_f^3	0.79	0.95	1.0	0.98	0.93	0.88	0.84	0.8	0.77	0.74
a_f^4	0.64	0.87	0.98	1.0	0.99	0.96	0.94	0.91	0.89	0.87
a_f^5	0.51	0.78	0.93	0.99	1.0	0.99	0.98	0.97	0.95	0.94
a_f^6	0.41	0.7	0.88	0.96	0.99	1.0	1.0	0.99	0.98	0.97
a_f^7	0.33	0.64	0.84	0.94	0.98	1.0	1.0	0.99	0.99	0.99
a_f^8	0.27	0.59	0.8	0.91	0.97	0.99	1.0	1.0	1.0	1.0
a_f^9	0.23	0.55	0.77	0.89	0.95	0.98	0.99	1.0	1.0	1.0
a_f^{10}	0.19	0.51	0.74	0.87	0.94	0.97	0.99	1.0	1.0	1.0

TABLE IV. Correlations among the a_f and a_g parameters.

	a_g^1	a_g^2	a_g^3	a_g^4	a_g^5	a_g^6	a_g^7	a_g^8	a_g^9	a_g^{10}
a_f^1	0.26	0.26	0.25	0.23	0.22	0.2	0.18	0.15	0.13	0.1
a_f^2	0.33	0.32	0.31	0.29	0.27	0.25	0.23	0.2	0.17	0.14
a_f^3	0.35	0.34	0.33	0.32	0.3	0.28	0.25	0.22	0.2	0.16
a_f^4	0.34	0.34	0.33	0.32	0.3	0.28	0.25	0.23	0.2	0.17
a_f^5	0.33	0.33	0.32	0.31	0.29	0.27	0.25	0.22	0.2	0.17
a_f^6	0.32	0.31	0.3	0.29	0.28	0.26	0.24	0.22	0.19	0.17
a_f^7	0.3	0.3	0.29	0.28	0.27	0.25	0.23	0.21	0.19	0.16
a_f^8	0.29	0.29	0.28	0.27	0.26	0.24	0.23	0.21	0.18	0.16
a_f^9	0.28	0.28	0.27	0.26	0.25	0.24	0.22	0.2	0.18	0.16
a_f^{10}	0.27	0.27	0.27	0.26	0.25	0.23	0.21	0.2	0.18	0.15

TABLE V. Correlations among the a_f and $a_{\mathcal{F}_1}$ parameters.

	$a_{\mathcal{F}_1}^1$	$a_{\mathcal{F}_1}^2$	$a_{\mathcal{F}_1}^3$	$a_{\mathcal{F}_1}^4$	$a_{\mathcal{F}_1}^5$	$a_{\mathcal{F}_1}^6$	$a_{\mathcal{F}_1}^7$	$a_{\mathcal{F}_1}^8$	$a_{\mathcal{F}_1}^9$	$a_{\mathcal{F}_1}^{10}$
a_f^1	0.72	0.71	0.65	0.58	0.52	0.47	0.42	0.37	0.33	0.3
a_f^2	0.66	0.67	0.64	0.59	0.53	0.49	0.44	0.4	0.35	0.31
a_f^3	0.54	0.57	0.56	0.53	0.49	0.46	0.42	0.38	0.33	0.29
a_f^4	0.41	0.47	0.48	0.46	0.44	0.41	0.37	0.34	0.3	0.26
a_f^5	0.32	0.38	0.4	0.4	0.38	0.36	0.33	0.3	0.27	0.23
a_f^6	0.24	0.31	0.34	0.34	0.34	0.32	0.3	0.27	0.24	0.21
a_f^7	0.18	0.25	0.29	0.3	0.3	0.29	0.27	0.25	0.22	0.19
a_f^8	0.14	0.21	0.25	0.27	0.27	0.26	0.25	0.23	0.2	0.17
a_f^9	0.1	0.18	0.22	0.24	0.25	0.24	0.23	0.21	0.19	0.16
a_f^{10}	0.07	0.15	0.2	0.22	0.23	0.23	0.21	0.2	0.17	0.15

TABLE VI. Correlations among the a_f and a_{P_1} parameters.

	$a_{P_1}^1$	$a_{P_1}^2$	$a_{P_1}^3$	$a_{P_1}^4$	$a_{P_1}^5$	$a_{P_1}^6$	$a_{P_1}^7$	$a_{P_1}^8$	$a_{P_1}^9$	$a_{P_1}^{10}$
a_f^1	0.61	0.6	0.59	0.57	0.55	0.52	0.48	0.44	0.39	0.34
a_f^2	0.6	0.61	0.6	0.59	0.58	0.56	0.53	0.5	0.46	0.42
a_f^3	0.54	0.55	0.55	0.55	0.54	0.52	0.5	0.47	0.44	
a_f^4	0.46	0.48	0.48	0.49	0.49	0.49	0.48	0.47	0.45	0.43
a_f^5	0.39	0.41	0.42	0.43	0.44	0.44	0.44	0.44	0.43	0.41
a_f^6	0.34	0.35	0.37	0.38	0.39	0.4	0.4	0.4	0.4	0.39
a_f^7	0.29	0.31	0.33	0.34	0.36	0.37	0.37	0.38	0.38	0.37
a_f^8	0.26	0.28	0.3	0.31	0.33	0.34	0.35	0.36	0.36	0.36
a_f^9	0.23	0.25	0.27	0.29	0.3	0.32	0.33	0.34	0.34	0.34
a_f^{10}	0.21	0.23	0.25	0.26	0.28	0.3	0.31	0.32	0.33	0.33

TABLE VII. Correlations among the a_f and b_f parameters.

	b_f^1	b_f^2	b_f^3	b_f^4	b_f^5	b_f^6	b_f^7	b_f^8	b_f^9	b_f^{10}
a_f^1	-0.99	-0.95	-0.82	-0.68	-0.56	-0.46	-0.39	-0.34	-0.29	-0.26
a_f^2	-0.91	-0.99	-0.96	-0.89	-0.81	-0.74	-0.68	-0.64	-0.6	-0.57
a_f^3	-0.75	-0.93	-0.99	-0.98	-0.94	-0.9	-0.87	-0.84	-0.81	-0.79
a_f^4	-0.59	-0.83	-0.95	-0.99	-0.99	-0.97	-0.95	-0.94	-0.92	-0.91
a_f^5	-0.45	-0.73	-0.9	-0.97	-0.99	-0.99	-0.99	-0.98	-0.97	-0.96
a_f^6	-0.35	-0.65	-0.84	-0.94	-0.98	-0.99	-1.0	-0.99	-0.99	-0.98
a_f^7	-0.27	-0.59	-0.8	-0.91	-0.96	-0.98	-0.99	-1.0	-1.0	-0.99
a_f^8	-0.21	-0.54	-0.76	-0.88	-0.94	-0.97	-0.99	-0.99	-1.0	-1.0
a_f^9	-0.16	-0.49	-0.73	-0.86	-0.93	-0.96	-0.98	-0.99	-0.99	-1.0
a_f^{10}	-0.12	-0.46	-0.7	-0.84	-0.91	-0.95	-0.97	-0.98	-0.99	-0.99

TABLE VIII. Correlations among the a_f and b_g parameters.

	b_g^1	b_g^2	b_g^3	b_g^4	b_g^5	b_g^6	b_g^7	b_g^8	b_g^9	b_g^{10}
a_f^1	-0.29	-0.28	-0.27	-0.26	-0.25	-0.24	-0.22	-0.21	-0.19	-0.18
a_f^2	-0.35	-0.34	-0.34	-0.32	-0.31	-0.3	-0.28	-0.26	-0.24	-0.23
a_f^3	-0.37	-0.36	-0.36	-0.34	-0.33	-0.32	-0.3	-0.28	-0.26	-0.24
a_f^4	-0.36	-0.36	-0.35	-0.34	-0.33	-0.31	-0.29	-0.28	-0.26	-0.24
a_f^5	-0.34	-0.34	-0.33	-0.33	-0.31	-0.3	-0.28	-0.27	-0.25	-0.23
a_f^6	-0.33	-0.32	-0.32	-0.31	-0.3	-0.29	-0.27	-0.26	-0.24	-0.23
a_f^7	-0.31	-0.31	-0.3	-0.3	-0.29	-0.27	-0.26	-0.25	-0.23	-0.22
a_f^8	-0.3	-0.3	-0.29	-0.28	-0.28	-0.26	-0.25	-0.24	-0.22	-0.21
a_f^9	-0.29	-0.29	-0.28	-0.27	-0.27	-0.25	-0.24	-0.23	-0.22	-0.2
a_f^{10}	-0.28	-0.28	-0.27	-0.27	-0.26	-0.25	-0.23	-0.22	-0.21	-0.2

TABLE IX. Correlations among the a_f and $b_{\mathcal{F}_1}$ parameters.

	$b_{\mathcal{F}_1}^1$	$b_{\mathcal{F}_1}^2$	$b_{\mathcal{F}_1}^3$	$b_{\mathcal{F}_1}^4$	$b_{\mathcal{F}_1}^5$	$b_{\mathcal{F}_1}^6$	$b_{\mathcal{F}_1}^7$	$b_{\mathcal{F}_1}^8$	$b_{\mathcal{F}_1}^9$	$b_{\mathcal{F}_1}^{10}$
a_f^1	-0.69	-0.67	-0.62	-0.56	-0.51	-0.47	-0.43	-0.4	-0.37	-0.34
a_f^2	-0.61	-0.62	-0.59	-0.54	-0.5	-0.47	-0.43	-0.4	-0.37	-0.34
a_f^3	-0.48	-0.51	-0.5	-0.48	-0.45	-0.42	-0.39	-0.37	-0.34	-0.31
a_f^4	-0.35	-0.4	-0.41	-0.4	-0.38	-0.36	-0.34	-0.32	-0.29	-0.26
a_f^5	-0.25	-0.31	-0.33	-0.33	-0.33	-0.31	-0.29	-0.27	-0.25	-0.23
a_f^6	-0.18	-0.24	-0.27	-0.28	-0.28	-0.27	-0.26	-0.24	-0.22	-0.19
a_f^7	-0.12	-0.19	-0.22	-0.24	-0.24	-0.24	-0.23	-0.21	-0.19	-0.17
a_f^8	-0.08	-0.15	-0.19	-0.21	-0.21	-0.21	-0.2	-0.19	-0.17	-0.15
a_f^9	-0.04	-0.11	-0.16	-0.18	-0.19	-0.19	-0.18	-0.17	-0.15	-0.14
a_f^{10}	-0.01	-0.09	-0.13	-0.16	-0.17	-0.17	-0.17	-0.16	-0.15	-0.14

TABLE X. Correlations among the a_f and b_{P_1} parameters.

	$b_{P_1}^1$	$b_{P_1}^2$	$b_{P_1}^3$	$b_{P_1}^4$	$b_{P_1}^5$	$b_{P_1}^6$	$b_{P_1}^7$	$b_{P_1}^8$	$b_{P_1}^9$	$b_{P_1}^{10}$
a_f^1	-0.61	-0.6	-0.59	-0.58	-0.56	-0.54	-0.51	-0.48	-0.46	-0.43
a_f^2	-0.59	-0.59	-0.58	-0.58	-0.56	-0.55	-0.53	-0.51	-0.49	-0.46
a_f^3	-0.51	-0.52	-0.52	-0.52	-0.51	-0.5	-0.49	-0.48	-0.46	-0.44
a_f^4	-0.43	-0.44	-0.44	-0.45	-0.45	-0.44	-0.44	-0.43	-0.42	-0.41
a_f^5	-0.36	-0.37	-0.38	-0.38	-0.38	-0.38	-0.38	-0.38	-0.37	-0.37
a_f^6	-0.3	-0.31	-0.32	-0.33	-0.33	-0.34	-0.34	-0.34	-0.34	-0.33
a_f^7	-0.25	-0.27	-0.28	-0.29	-0.3	-0.3	-0.3	-0.31	-0.31	-0.3
a_f^8	-0.22	-0.23	-0.24	-0.25	-0.26	-0.27	-0.28	-0.28	-0.28	-0.28
a_f^9	-0.19	-0.2	-0.22	-0.23	-0.24	-0.25	-0.25	-0.26	-0.26	-0.26
a_f^{10}	-0.16	-0.18	-0.19	-0.21	-0.22	-0.23	-0.23	-0.24	-0.24	-0.25

TABLE XI. Correlations among the a_g and a_g parameters.

	a_g^1	a_g^2	a_g^3	a_g^4	a_g^5	a_g^6	a_g^7	a_g^8	a_g^9	a_g^{10}
a_g^1	1.0	1.0	0.98	0.96	0.92	0.87	0.82	0.76	0.69	0.61
a_g^2	1.0	1.0	0.99	0.98	0.95	0.92	0.87	0.82	0.75	0.69
a_g^3	0.98	0.99	1.0	0.99	0.98	0.95	0.91	0.87	0.82	0.76
a_g^4	0.96	0.98	0.99	1.0	0.99	0.98	0.95	0.92	0.87	0.82
a_g^5	0.92	0.95	0.98	0.99	1.0	0.99	0.98	0.95	0.92	0.87
a_g^6	0.87	0.92	0.95	0.98	0.99	1.0	0.99	0.98	0.95	0.92
a_g^7	0.82	0.87	0.91	0.95	0.98	0.99	1.0	0.99	0.98	0.96
a_g^8	0.76	0.82	0.87	0.92	0.95	0.98	0.99	1.0	1.0	0.98
a_g^9	0.69	0.75	0.82	0.87	0.92	0.95	0.98	1.0	1.0	1.0
a_g^{10}	0.61	0.69	0.76	0.82	0.87	0.92	0.96	0.98	1.0	1.0

TABLE XII. Correlations among the a_g and $a_{\mathcal{F}_1}$ parameters.

	$a_{\mathcal{F}_1}^1$	$a_{\mathcal{F}_1}^2$	$a_{\mathcal{F}_1}^3$	$a_{\mathcal{F}_1}^4$	$a_{\mathcal{F}_1}^5$	$a_{\mathcal{F}_1}^6$	$a_{\mathcal{F}_1}^7$	$a_{\mathcal{F}_1}^8$	$a_{\mathcal{F}_1}^9$	$a_{\mathcal{F}_1}^{10}$
a_g^1	0.12	0.18	0.23	0.27	0.29	0.3	0.3	0.3	0.29	0.28
a_g^2	0.11	0.18	0.23	0.26	0.28	0.29	0.3	0.3	0.29	0.28
a_g^3	0.1	0.17	0.22	0.25	0.27	0.29	0.29	0.29	0.28	0.27
a_g^4	0.09	0.16	0.21	0.24	0.26	0.28	0.28	0.28	0.27	0.26
a_g^5	0.09	0.15	0.2	0.23	0.25	0.26	0.27	0.26	0.26	0.25
a_g^6	0.07	0.14	0.18	0.21	0.23	0.24	0.25	0.25	0.24	0.23
a_g^7	0.06	0.12	0.17	0.19	0.21	0.22	0.23	0.23	0.22	0.21
a_g^8	0.05	0.1	0.15	0.17	0.19	0.2	0.2	0.2	0.2	0.19
a_g^9	0.04	0.09	0.12	0.15	0.16	0.17	0.18	0.18	0.17	0.16
a_g^{10}	0.02	0.07	0.1	0.12	0.14	0.15	0.15	0.15	0.14	0.14

TABLE XIII. Correlations among the a_g and a_{P_1} parameters.

	$a_{P_1}^1$	$a_{P_1}^2$	$a_{P_1}^3$	$a_{P_1}^4$	$a_{P_1}^5$	$a_{P_1}^6$	$a_{P_1}^7$	$a_{P_1}^8$	$a_{P_1}^9$	$a_{P_1}^{10}$
a_g^1	0.41	0.41	0.41	0.4	0.39	0.38	0.36	0.33	0.31	0.27
a_g^2	0.41	0.41	0.41	0.4	0.39	0.38	0.36	0.33	0.31	0.28
a_g^3	0.4	0.4	0.4	0.39	0.38	0.37	0.35	0.33	0.3	0.27
a_g^4	0.39	0.39	0.39	0.38	0.38	0.36	0.34	0.32	0.3	0.27
a_g^5	0.37	0.38	0.37	0.37	0.36	0.35	0.33	0.31	0.29	0.26
a_g^6	0.35	0.36	0.35	0.35	0.34	0.33	0.32	0.3	0.28	0.25
a_g^7	0.33	0.33	0.33	0.33	0.32	0.31	0.3	0.28	0.26	0.24
a_g^8	0.3	0.3	0.3	0.3	0.3	0.29	0.28	0.26	0.25	0.23
a_g^9	0.27	0.28	0.28	0.27	0.27	0.26	0.26	0.24	0.23	0.21
a_g^{10}	0.24	0.24	0.24	0.24	0.24	0.24	0.23	0.22	0.21	0.19

TABLE XIV. Correlations among the a_g and b_f parameters.

	b_f^1	b_f^2	b_f^3	b_f^4	b_f^5	b_f^6	b_f^7	b_f^8	b_f^9	b_f^{10}
a_g^1	-0.26	-0.33	-0.36	-0.36	-0.35	-0.34	-0.32	-0.31	-0.31	-0.3
a_g^2	-0.26	-0.33	-0.35	-0.35	-0.34	-0.33	-0.32	-0.31	-0.3	-0.3
a_g^3	-0.25	-0.32	-0.34	-0.34	-0.34	-0.32	-0.31	-0.3	-0.3	-0.29
a_g^4	-0.23	-0.3	-0.33	-0.33	-0.32	-0.31	-0.3	-0.29	-0.29	-0.28
a_g^5	-0.22	-0.28	-0.31	-0.31	-0.31	-0.3	-0.29	-0.28	-0.27	-0.27
a_g^6	-0.2	-0.26	-0.29	-0.29	-0.29	-0.28	-0.27	-0.26	-0.26	-0.25
a_g^7	-0.18	-0.23	-0.26	-0.27	-0.26	-0.26	-0.25	-0.24	-0.24	-0.23
a_g^8	-0.15	-0.21	-0.23	-0.24	-0.24	-0.23	-0.23	-0.22	-0.22	-0.21
a_g^9	-0.13	-0.18	-0.2	-0.21	-0.21	-0.2	-0.2	-0.2	-0.19	-0.19
a_g^{10}	-0.1	-0.15	-0.17	-0.18	-0.18	-0.18	-0.17	-0.17	-0.17	-0.17

TABLE XV. Correlations among the a_g and b_g parameters.

	b_g^1	b_g^2	b_g^3	b_g^4	b_g^5	b_g^6	b_g^7	b_g^8	b_g^9	b_g^{10}
a_g^1	-0.99	-0.98	-0.97	-0.95	-0.92	-0.88	-0.84	-0.79	-0.75	-0.7
a_g^2	-0.98	-0.99	-0.98	-0.97	-0.94	-0.92	-0.88	-0.84	-0.8	-0.76
a_g^3	-0.96	-0.98	-0.98	-0.98	-0.97	-0.94	-0.92	-0.89	-0.85	-0.82
a_g^4	-0.93	-0.96	-0.97	-0.98	-0.98	-0.96	-0.95	-0.92	-0.9	-0.87
a_g^5	-0.89	-0.93	-0.95	-0.97	-0.97	-0.97	-0.96	-0.95	-0.93	-0.91
a_g^6	-0.84	-0.89	-0.92	-0.95	-0.96	-0.97	-0.97	-0.96	-0.95	-0.94
a_g^7	-0.78	-0.84	-0.88	-0.91	-0.94	-0.96	-0.96	-0.97	-0.96	-0.95
a_g^8	-0.72	-0.78	-0.83	-0.87	-0.91	-0.93	-0.95	-0.96	-0.96	-0.96
a_g^9	-0.64	-0.71	-0.77	-0.82	-0.87	-0.9	-0.92	-0.94	-0.95	-0.96
a_g^{10}	-0.57	-0.64	-0.71	-0.77	-0.82	-0.86	-0.89	-0.91	-0.93	-0.94

TABLE XVI. Correlations among the a_g and $b_{\mathcal{F}_1}$ parameters.

	$b_{\mathcal{F}_1}^1$	$b_{\mathcal{F}_1}^2$	$b_{\mathcal{F}_1}^3$	$b_{\mathcal{F}_1}^4$	$b_{\mathcal{F}_1}^5$	$b_{\mathcal{F}_1}^6$	$b_{\mathcal{F}_1}^7$	$b_{\mathcal{F}_1}^8$	$b_{\mathcal{F}_1}^9$	$b_{\mathcal{F}_1}^{10}$
a_g^1	-0.11	-0.17	-0.22	-0.25	-0.27	-0.28	-0.29	-0.29	-0.29	-0.28
a_g^2	-0.1	-0.17	-0.22	-0.25	-0.27	-0.28	-0.28	-0.29	-0.28	-0.28
a_g^3	-0.1	-0.16	-0.21	-0.24	-0.26	-0.27	-0.28	-0.28	-0.28	-0.27
a_g^4	-0.09	-0.15	-0.2	-0.23	-0.25	-0.26	-0.27	-0.27	-0.27	-0.26
a_g^5	-0.08	-0.14	-0.19	-0.22	-0.24	-0.25	-0.25	-0.25	-0.25	-0.25
a_g^6	-0.07	-0.13	-0.17	-0.2	-0.22	-0.23	-0.24	-0.24	-0.23	-0.23
a_g^7	-0.06	-0.11	-0.16	-0.18	-0.2	-0.21	-0.22	-0.22	-0.21	-0.21
a_g^8	-0.04	-0.1	-0.14	-0.16	-0.18	-0.19	-0.19	-0.19	-0.19	-0.19
a_g^9	-0.03	-0.08	-0.12	-0.14	-0.15	-0.16	-0.17	-0.17	-0.17	-0.16
a_g^{10}	-0.02	-0.06	-0.09	-0.11	-0.13	-0.14	-0.14	-0.14	-0.14	-0.14

TABLE XVII. Correlations among the a_g and b_{P_1} parameters.

	$b_{P_1}^1$	$b_{P_1}^2$	$b_{P_1}^3$	$b_{P_1}^4$	$b_{P_1}^5$	$b_{P_1}^6$	$b_{P_1}^7$	$b_{P_1}^8$	$b_{P_1}^9$	$b_{P_1}^{10}$
a_g^1	-0.4	-0.4	-0.39	-0.39	-0.38	-0.36	-0.35	-0.34	-0.32	-0.3
a_g^2	-0.4	-0.4	-0.39	-0.38	-0.38	-0.36	-0.35	-0.33	-0.32	-0.3
a_g^3	-0.39	-0.39	-0.38	-0.38	-0.37	-0.36	-0.34	-0.33	-0.31	-0.3
a_g^4	-0.38	-0.38	-0.37	-0.37	-0.36	-0.35	-0.34	-0.32	-0.31	-0.29
a_g^5	-0.36	-0.36	-0.36	-0.35	-0.34	-0.33	-0.32	-0.31	-0.3	-0.28
a_g^6	-0.34	-0.34	-0.34	-0.33	-0.33	-0.32	-0.31	-0.29	-0.28	-0.27
a_g^7	-0.31	-0.31	-0.31	-0.31	-0.3	-0.29	-0.29	-0.27	-0.26	-0.25
a_g^8	-0.29	-0.29	-0.29	-0.28	-0.28	-0.27	-0.26	-0.25	-0.24	-0.23
a_g^9	-0.26	-0.26	-0.26	-0.25	-0.25	-0.24	-0.24	-0.23	-0.22	-0.21
a_g^{10}	-0.22	-0.22	-0.22	-0.22	-0.22	-0.21	-0.21	-0.2	-0.19	-0.19

TABLE XVIII. Correlations among the $a_{\mathcal{F}_1}$ and $a_{\mathcal{F}_1}$ parameters.

	$a_{\mathcal{F}_1}^1$	$a_{\mathcal{F}_1}^2$	$a_{\mathcal{F}_1}^3$	$a_{\mathcal{F}_1}^4$	$a_{\mathcal{F}_1}^5$	$a_{\mathcal{F}_1}^6$	$a_{\mathcal{F}_1}^7$	$a_{\mathcal{F}_1}^8$	$a_{\mathcal{F}_1}^9$	$a_{\mathcal{F}_1}^{10}$
$a_{\mathcal{F}_1}^1$	1.0	0.95	0.85	0.74	0.64	0.55	0.48	0.41	0.36	0.31
$a_{\mathcal{F}_1}^2$	0.95	1.0	0.97	0.9	0.83	0.76	0.69	0.61	0.54	0.47
$a_{\mathcal{F}_1}^3$	0.85	0.97	1.0	0.98	0.94	0.89	0.83	0.76	0.68	0.6
$a_{\mathcal{F}_1}^4$	0.74	0.9	0.98	1.0	0.99	0.96	0.91	0.85	0.79	0.71
$a_{\mathcal{F}_1}^5$	0.64	0.83	0.94	0.99	1.0	0.99	0.96	0.92	0.86	0.79
$a_{\mathcal{F}_1}^6$	0.55	0.76	0.89	0.96	0.99	1.0	0.99	0.96	0.92	0.87
$a_{\mathcal{F}_1}^7$	0.48	0.69	0.83	0.91	0.96	0.99	1.0	0.99	0.97	0.92
$a_{\mathcal{F}_1}^8$	0.41	0.61	0.76	0.85	0.92	0.96	0.99	1.0	0.99	0.97
$a_{\mathcal{F}_1}^9$	0.36	0.54	0.68	0.79	0.86	0.92	0.97	0.99	1.0	0.99
$a_{\mathcal{F}_1}^{10}$	0.31	0.47	0.6	0.71	0.79	0.87	0.92	0.97	0.99	1.0

TABLE XIX. Correlations among the a_{F_1} and a_{P_1} parameters.

	$a_{P_1}^1$	$a_{P_1}^2$	$a_{P_1}^3$	$a_{P_1}^4$	$a_{P_1}^5$	$a_{P_1}^6$	$a_{P_1}^7$	$a_{P_1}^8$	$a_{P_1}^9$	$a_{P_1}^{10}$
$a_{F_1}^1$	0.51	0.5	0.48	0.46	0.42	0.39	0.34	0.29	0.24	0.18
$a_{F_1}^2$	0.65	0.64	0.63	0.61	0.58	0.55	0.5	0.45	0.4	0.34
$a_{F_1}^3$	0.72	0.72	0.72	0.71	0.68	0.65	0.62	0.57	0.51	0.45
$a_{F_1}^4$	0.76	0.76	0.77	0.76	0.74	0.72	0.69	0.64	0.59	0.53
$a_{F_1}^5$	0.77	0.78	0.79	0.79	0.78	0.76	0.73	0.69	0.64	0.59
$a_{F_1}^6$	0.77	0.78	0.8	0.8	0.79	0.78	0.76	0.72	0.68	0.63
$a_{F_1}^7$	0.75	0.77	0.79	0.8	0.8	0.79	0.77	0.74	0.7	0.65
$a_{F_1}^8$	0.73	0.75	0.77	0.78	0.79	0.78	0.77	0.74	0.71	0.66
$a_{F_1}^9$	0.7	0.72	0.74	0.76	0.76	0.76	0.75	0.73	0.7	0.66
$a_{F_1}^{10}$	0.66	0.68	0.7	0.72	0.73	0.73	0.72	0.71	0.68	0.64

TABLE XX. Correlations among the a_{F_1} and b_f parameters.

	b_f^1	b_f^2	b_f^3	b_f^4	b_f^5	b_f^6	b_f^7	b_f^8	b_f^9	b_f^{10}
$a_{F_1}^1$	-0.71	-0.66	-0.55	-0.44	-0.35	-0.28	-0.22	-0.18	-0.15	-0.12
$a_{F_1}^2$	-0.71	-0.69	-0.6	-0.5	-0.42	-0.35	-0.3	-0.26	-0.23	-0.2
$a_{F_1}^3$	-0.66	-0.66	-0.6	-0.51	-0.44	-0.38	-0.34	-0.3	-0.28	-0.25
$a_{F_1}^4$	-0.6	-0.61	-0.57	-0.5	-0.44	-0.39	-0.35	-0.32	-0.3	-0.28
$a_{F_1}^5$	-0.54	-0.56	-0.53	-0.48	-0.43	-0.38	-0.35	-0.32	-0.3	-0.28
$a_{F_1}^6$	-0.48	-0.52	-0.49	-0.45	-0.4	-0.37	-0.34	-0.31	-0.29	-0.28
$a_{F_1}^7$	-0.44	-0.47	-0.45	-0.41	-0.38	-0.34	-0.32	-0.29	-0.28	-0.26
$a_{F_1}^8$	-0.39	-0.43	-0.41	-0.38	-0.34	-0.31	-0.29	-0.27	-0.25	-0.24
$a_{F_1}^9$	-0.35	-0.38	-0.37	-0.34	-0.31	-0.28	-0.26	-0.24	-0.23	-0.21
$a_{F_1}^{10}$	-0.31	-0.34	-0.32	-0.29	-0.27	-0.24	-0.22	-0.21	-0.19	-0.18

TABLE XXI. Correlations among the a_{F_1} and b_g parameters.

	b_g^1	b_g^2	b_g^3	b_g^4	b_g^5	b_g^6	b_g^7	b_g^8	b_g^9	b_g^{10}
$a_{F_1}^1$	-0.14	-0.14	-0.14	-0.13	-0.13	-0.12	-0.11	-0.1	-0.1	-0.09
$a_{F_1}^2$	-0.22	-0.22	-0.21	-0.21	-0.2	-0.19	-0.19	-0.18	-0.17	-0.16
$a_{F_1}^3$	-0.27	-0.27	-0.27	-0.26	-0.26	-0.25	-0.24	-0.23	-0.21	-0.2
$a_{F_1}^4$	-0.3	-0.3	-0.3	-0.3	-0.29	-0.28	-0.27	-0.26	-0.25	-0.23
$a_{F_1}^5$	-0.32	-0.33	-0.32	-0.32	-0.31	-0.3	-0.29	-0.28	-0.27	-0.25
$a_{F_1}^6$	-0.34	-0.34	-0.34	-0.33	-0.32	-0.31	-0.3	-0.29	-0.28	-0.26
$a_{F_1}^7$	-0.34	-0.34	-0.34	-0.34	-0.33	-0.32	-0.31	-0.29	-0.28	-0.26
$a_{F_1}^8$	-0.34	-0.34	-0.34	-0.33	-0.33	-0.32	-0.3	-0.29	-0.28	-0.26
$a_{F_1}^9$	-0.33	-0.33	-0.33	-0.33	-0.32	-0.31	-0.3	-0.28	-0.27	-0.25
$a_{F_1}^{10}$	-0.32	-0.32	-0.32	-0.31	-0.3	-0.29	-0.28	-0.27	-0.26	-0.24

TABLE XXII. Correlations among the $a_{\mathcal{F}_1}$ and $b_{\mathcal{F}_1}$ parameters.

	$b_{\mathcal{F}_1}^1$	$b_{\mathcal{F}_1}^2$	$b_{\mathcal{F}_1}^3$	$b_{\mathcal{F}_1}^4$	$b_{\mathcal{F}_1}^5$	$b_{\mathcal{F}_1}^6$	$b_{\mathcal{F}_1}^7$	$b_{\mathcal{F}_1}^8$	$b_{\mathcal{F}_1}^9$	$b_{\mathcal{F}_1}^{10}$
$a_{\mathcal{F}_1}^1$	-0.99	-0.94	-0.84	-0.74	-0.66	-0.59	-0.53	-0.48	-0.43	-0.39
$a_{\mathcal{F}_1}^2$	-0.95	-0.99	-0.96	-0.9	-0.84	-0.79	-0.73	-0.67	-0.62	-0.56
$a_{\mathcal{F}_1}^3$	-0.85	-0.96	-0.99	-0.98	-0.94	-0.9	-0.86	-0.81	-0.75	-0.69
$a_{\mathcal{F}_1}^4$	-0.74	-0.9	-0.97	-0.99	-0.99	-0.96	-0.93	-0.89	-0.84	-0.79
$a_{\mathcal{F}_1}^5$	-0.65	-0.83	-0.93	-0.98	-0.99	-0.99	-0.97	-0.95	-0.91	-0.86
$a_{\mathcal{F}_1}^6$	-0.56	-0.76	-0.88	-0.94	-0.98	-0.99	-0.99	-0.98	-0.95	-0.92
$a_{\mathcal{F}_1}^7$	-0.49	-0.69	-0.82	-0.9	-0.95	-0.98	-0.99	-0.99	-0.98	-0.96
$a_{\mathcal{F}_1}^8$	-0.43	-0.62	-0.75	-0.84	-0.9	-0.95	-0.97	-0.99	-0.99	-0.99
$a_{\mathcal{F}_1}^9$	-0.37	-0.55	-0.68	-0.77	-0.84	-0.9	-0.94	-0.97	-0.99	-0.99
$a_{\mathcal{F}_1}^{10}$	-0.32	-0.48	-0.6	-0.7	-0.77	-0.84	-0.89	-0.94	-0.97	-0.99

TABLE XXIII. Correlations among the $a_{\mathcal{F}_1}$ and b_{P_1} parameters.

	$b_{P_1}^1$	$b_{P_1}^2$	$b_{P_1}^3$	$b_{P_1}^4$	$b_{P_1}^5$	$b_{P_1}^6$	$b_{P_1}^7$	$b_{P_1}^8$	$b_{P_1}^9$	$b_{P_1}^{10}$
$a_{\mathcal{F}_1}^1$	-0.57	-0.57	-0.56	-0.54	-0.52	-0.5	-0.48	-0.45	-0.43	-0.4
$a_{\mathcal{F}_1}^2$	-0.72	-0.72	-0.72	-0.71	-0.7	-0.68	-0.66	-0.64	-0.61	-0.58
$a_{\mathcal{F}_1}^3$	-0.79	-0.81	-0.81	-0.81	-0.8	-0.79	-0.78	-0.76	-0.74	-0.71
$a_{\mathcal{F}_1}^4$	-0.83	-0.85	-0.86	-0.86	-0.86	-0.86	-0.85	-0.83	-0.81	-0.79
$a_{\mathcal{F}_1}^5$	-0.84	-0.86	-0.88	-0.89	-0.89	-0.89	-0.89	-0.87	-0.86	-0.84
$a_{\mathcal{F}_1}^6$	-0.83	-0.86	-0.88	-0.9	-0.91	-0.91	-0.91	-0.9	-0.88	-0.87
$a_{\mathcal{F}_1}^7$	-0.82	-0.85	-0.87	-0.89	-0.9	-0.91	-0.91	-0.9	-0.89	-0.88
$a_{\mathcal{F}_1}^8$	-0.79	-0.82	-0.85	-0.87	-0.89	-0.89	-0.9	-0.89	-0.89	-0.88
$a_{\mathcal{F}_1}^9$	-0.75	-0.79	-0.82	-0.84	-0.86	-0.87	-0.87	-0.87	-0.87	-0.86
$a_{\mathcal{F}_1}^{10}$	-0.71	-0.74	-0.77	-0.79	-0.81	-0.82	-0.83	-0.83	-0.83	-0.82

TABLE XXIV. Correlations among the a_{P_1} and a_{P_1} parameters.

	$a_{P_1}^1$	$a_{P_1}^2$	$a_{P_1}^3$	$a_{P_1}^4$	$a_{P_1}^5$	$a_{P_1}^6$	$a_{P_1}^7$	$a_{P_1}^8$	$a_{P_1}^9$	$a_{P_1}^{10}$
$a_{P_1}^1$	1.0	1.0	0.99	0.97	0.94	0.89	0.84	0.78	0.71	0.63
$a_{P_1}^2$	1.0	1.0	1.0	0.98	0.96	0.93	0.89	0.83	0.77	0.7
$a_{P_1}^3$	0.99	1.0	1.0	1.0	0.98	0.96	0.92	0.88	0.82	0.76
$a_{P_1}^4$	0.97	0.98	1.0	1.0	1.0	0.98	0.95	0.92	0.87	0.81
$a_{P_1}^5$	0.94	0.96	0.98	1.0	1.0	0.99	0.98	0.95	0.92	0.87
$a_{P_1}^6$	0.89	0.93	0.96	0.98	0.99	1.0	0.99	0.98	0.95	0.91
$a_{P_1}^7$	0.84	0.89	0.92	0.95	0.98	0.99	1.0	0.99	0.98	0.95
$a_{P_1}^8$	0.78	0.83	0.88	0.92	0.95	0.98	0.99	1.0	0.99	0.98
$a_{P_1}^9$	0.71	0.77	0.82	0.87	0.92	0.95	0.98	0.99	1.0	0.99
$a_{P_1}^{10}$	0.63	0.7	0.76	0.81	0.87	0.91	0.95	0.98	0.99	1.0

TABLE XXV. Correlations among the a_{P_1} and b_f parameters.

	b_f^1	b_f^2	b_f^3	b_f^4	b_f^5	b_f^6	b_f^7	b_f^8	b_f^9	b_f^{10}
$a_{P_1}^1$	-0.6	-0.61	-0.55	-0.48	-0.42	-0.37	-0.33	-0.3	-0.27	-0.25
$a_{P_1}^2$	-0.59	-0.61	-0.56	-0.5	-0.43	-0.39	-0.35	-0.32	-0.29	-0.27
$a_{P_1}^3$	-0.58	-0.6	-0.56	-0.5	-0.45	-0.4	-0.36	-0.33	-0.31	-0.29
$a_{P_1}^4$	-0.56	-0.59	-0.56	-0.51	-0.45	-0.41	-0.38	-0.35	-0.32	-0.31
$a_{P_1}^5$	-0.53	-0.58	-0.55	-0.51	-0.46	-0.42	-0.39	-0.36	-0.34	-0.32
$a_{P_1}^6$	-0.5	-0.55	-0.54	-0.5	-0.46	-0.42	-0.39	-0.37	-0.35	-0.33
$a_{P_1}^7$	-0.47	-0.52	-0.52	-0.49	-0.46	-0.42	-0.4	-0.38	-0.36	-0.34
$a_{P_1}^8$	-0.42	-0.49	-0.5	-0.48	-0.45	-0.42	-0.4	-0.38	-0.36	-0.35
$a_{P_1}^9$	-0.37	-0.45	-0.47	-0.45	-0.43	-0.41	-0.39	-0.38	-0.36	-0.35
$a_{P_1}^{10}$	-0.32	-0.4	-0.43	-0.43	-0.41	-0.4	-0.38	-0.37	-0.36	-0.35

TABLE XXVI. Correlations among the a_{P_1} and b_g parameters.

	b_g^1	b_g^2	b_g^3	b_g^4	b_g^5	b_g^6	b_g^7	b_g^8	b_g^9	b_g^{10}
$a_{P_1}^1$	-0.42	-0.42	-0.41	-0.41	-0.39	-0.38	-0.36	-0.34	-0.32	-0.3
$a_{P_1}^2$	-0.42	-0.42	-0.41	-0.4	-0.39	-0.38	-0.36	-0.34	-0.32	-0.3
$a_{P_1}^3$	-0.41	-0.41	-0.41	-0.4	-0.39	-0.37	-0.36	-0.34	-0.32	-0.3
$a_{P_1}^4$	-0.41	-0.41	-0.4	-0.39	-0.38	-0.37	-0.35	-0.33	-0.32	-0.3
$a_{P_1}^5$	-0.39	-0.39	-0.39	-0.38	-0.37	-0.36	-0.34	-0.32	-0.31	-0.29
$a_{P_1}^6$	-0.38	-0.38	-0.37	-0.37	-0.36	-0.34	-0.33	-0.31	-0.3	-0.28
$a_{P_1}^7$	-0.35	-0.36	-0.35	-0.35	-0.34	-0.32	-0.31	-0.3	-0.28	-0.27
$a_{P_1}^8$	-0.33	-0.33	-0.33	-0.32	-0.31	-0.3	-0.29	-0.28	-0.26	-0.25
$a_{P_1}^9$	-0.3	-0.3	-0.3	-0.29	-0.29	-0.28	-0.27	-0.25	-0.24	-0.23
$a_{P_1}^{10}$	-0.27	-0.27	-0.27	-0.26	-0.26	-0.25	-0.24	-0.23	-0.22	-0.21

TABLE XXVII. Correlations among the a_{P_1} and $b_{\mathcal{F}_1}$ parameters.

	$b_{\mathcal{F}_1}^1$	$b_{\mathcal{F}_1}^2$	$b_{\mathcal{F}_1}^3$	$b_{\mathcal{F}_1}^4$	$b_{\mathcal{F}_1}^5$	$b_{\mathcal{F}_1}^6$	$b_{\mathcal{F}_1}^7$	$b_{\mathcal{F}_1}^8$	$b_{\mathcal{F}_1}^9$	$b_{\mathcal{F}_1}^{10}$
$a_{P_1}^1$	-0.5	-0.62	-0.69	-0.72	-0.74	-0.74	-0.74	-0.73	-0.71	-0.68
$a_{P_1}^2$	-0.48	-0.62	-0.69	-0.73	-0.75	-0.76	-0.76	-0.75	-0.73	-0.7
$a_{P_1}^3$	-0.46	-0.6	-0.68	-0.73	-0.75	-0.76	-0.77	-0.76	-0.74	-0.72
$a_{P_1}^4$	-0.43	-0.58	-0.67	-0.72	-0.75	-0.76	-0.77	-0.77	-0.75	-0.73
$a_{P_1}^5$	-0.4	-0.55	-0.65	-0.7	-0.74	-0.76	-0.77	-0.77	-0.76	-0.74
$a_{P_1}^6$	-0.36	-0.52	-0.62	-0.68	-0.72	-0.74	-0.75	-0.76	-0.75	-0.73
$a_{P_1}^7$	-0.32	-0.47	-0.58	-0.64	-0.68	-0.71	-0.73	-0.74	-0.73	-0.72
$a_{P_1}^8$	-0.27	-0.42	-0.53	-0.6	-0.64	-0.68	-0.7	-0.71	-0.71	-0.7
$a_{P_1}^9$	-0.21	-0.36	-0.47	-0.54	-0.6	-0.63	-0.65	-0.67	-0.67	-0.66
$a_{P_1}^{10}$	-0.16	-0.3	-0.41	-0.48	-0.54	-0.58	-0.6	-0.62	-0.62	-0.62

TABLE XXVIII. Correlations among the a_{P_1} and b_{P_1} parameters.

	$b_{P_1}^1$	$b_{P_1}^2$	$b_{P_1}^3$	$b_{P_1}^4$	$b_{P_1}^5$	$b_{P_1}^6$	$b_{P_1}^7$	$b_{P_1}^8$	$b_{P_1}^9$	$b_{P_1}^{10}$
$a_{P_1}^1$	-0.99	-0.98	-0.97	-0.95	-0.93	-0.9	-0.87	-0.83	-0.79	-0.74
$a_{P_1}^2$	-0.98	-0.98	-0.98	-0.97	-0.95	-0.93	-0.9	-0.87	-0.83	-0.79
$a_{P_1}^3$	-0.96	-0.97	-0.98	-0.97	-0.96	-0.95	-0.92	-0.9	-0.87	-0.84
$a_{P_1}^4$	-0.94	-0.96	-0.97	-0.97	-0.97	-0.96	-0.95	-0.93	-0.9	-0.87
$a_{P_1}^5$	-0.91	-0.93	-0.95	-0.96	-0.97	-0.96	-0.96	-0.94	-0.93	-0.91
$a_{P_1}^6$	-0.86	-0.89	-0.92	-0.94	-0.95	-0.96	-0.96	-0.95	-0.94	-0.93
$a_{P_1}^7$	-0.81	-0.85	-0.88	-0.91	-0.93	-0.94	-0.95	-0.95	-0.95	-0.94
$a_{P_1}^8$	-0.74	-0.79	-0.83	-0.86	-0.89	-0.92	-0.93	-0.94	-0.94	-0.94
$a_{P_1}^9$	-0.67	-0.72	-0.77	-0.81	-0.85	-0.88	-0.9	-0.92	-0.93	-0.93
$a_{P_1}^{10}$	-0.58	-0.64	-0.7	-0.75	-0.79	-0.83	-0.86	-0.88	-0.9	-0.91

TABLE XXIX. Correlations among the b_f and b_g parameters.

	b_f^1	b_f^2	b_f^3	b_f^4	b_f^5	b_f^6	b_f^7	b_f^8	b_f^9	b_f^{10}
b_f^1	1.0	0.94	0.79	0.64	0.52	0.42	0.35	0.29	0.25	0.21
b_f^2	0.94	1.0	0.96	0.87	0.78	0.71	0.65	0.6	0.57	0.53
b_f^3	0.79	0.96	1.0	0.98	0.93	0.89	0.85	0.81	0.78	0.76
b_f^4	0.64	0.87	0.98	1.0	0.99	0.97	0.94	0.92	0.9	0.88
b_f^5	0.52	0.78	0.93	0.99	1.0	0.99	0.98	0.97	0.96	0.95
b_f^6	0.42	0.71	0.89	0.97	0.99	1.0	1.0	0.99	0.98	0.98
b_f^7	0.35	0.65	0.85	0.94	0.98	1.0	1.0	1.0	0.99	0.99
b_f^8	0.29	0.6	0.81	0.92	0.97	0.99	1.0	1.0	1.0	1.0
b_f^9	0.25	0.57	0.78	0.9	0.96	0.98	0.99	1.0	1.0	1.0
b_f^{10}	0.21	0.53	0.76	0.88	0.95	0.98	0.99	1.0	1.0	1.0

TABLE XXX. Correlations among the b_f and b_g parameters.

	b_g^1	b_g^2	b_g^3	b_g^4	b_g^5	b_g^6	b_g^7	b_g^8	b_g^9	b_g^{10}
b_f^1	0.29	0.29	0.28	0.27	0.26	0.25	0.23	0.22	0.2	0.19
b_f^2	0.36	0.36	0.35	0.34	0.33	0.31	0.29	0.28	0.26	0.24
b_f^3	0.38	0.38	0.37	0.36	0.35	0.33	0.32	0.3	0.28	0.26
b_f^4	0.38	0.38	0.37	0.36	0.35	0.33	0.32	0.3	0.28	0.26
b_f^5	0.37	0.36	0.36	0.35	0.34	0.32	0.31	0.29	0.27	0.25
b_f^6	0.35	0.35	0.34	0.34	0.32	0.31	0.3	0.28	0.26	0.25
b_f^7	0.34	0.34	0.33	0.32	0.31	0.3	0.28	0.27	0.25	0.24
b_f^8	0.33	0.32	0.32	0.31	0.3	0.29	0.28	0.26	0.25	0.23
b_f^9	0.32	0.32	0.31	0.3	0.29	0.28	0.27	0.25	0.24	0.22
b_f^{10}	0.31	0.31	0.3	0.3	0.29	0.27	0.26	0.25	0.23	0.22

TABLE XXXI. Correlations among the b_f and $b_{\mathcal{F}_1}$ parameters.

	$b_{\mathcal{F}_1}^1$	$b_{\mathcal{F}_1}^2$	$b_{\mathcal{F}_1}^3$	$b_{\mathcal{F}_1}^4$	$b_{\mathcal{F}_1}^5$	$b_{\mathcal{F}_1}^6$	$b_{\mathcal{F}_1}^7$	$b_{\mathcal{F}_1}^8$	$b_{\mathcal{F}_1}^9$	$b_{\mathcal{F}_1}^{10}$
b_f^1	0.7	0.69	0.64	0.59	0.54	0.5	0.46	0.43	0.4	0.37
b_f^2	0.63	0.65	0.63	0.59	0.55	0.51	0.48	0.45	0.41	0.38
b_f^3	0.51	0.55	0.55	0.53	0.5	0.47	0.44	0.41	0.38	0.35
b_f^4	0.39	0.45	0.46	0.46	0.44	0.42	0.39	0.37	0.34	0.31
b_f^5	0.3	0.36	0.39	0.39	0.38	0.37	0.35	0.33	0.3	0.27
b_f^6	0.23	0.3	0.33	0.34	0.34	0.33	0.31	0.29	0.27	0.24
b_f^7	0.17	0.25	0.28	0.3	0.3	0.29	0.28	0.26	0.24	0.22
b_f^8	0.13	0.21	0.25	0.27	0.27	0.27	0.26	0.24	0.22	0.2
b_f^9	0.1	0.18	0.22	0.24	0.25	0.25	0.24	0.22	0.2	0.18
b_f^{10}	0.07	0.15	0.2	0.22	0.23	0.23	0.22	0.21	0.19	0.17

TABLE XXXII. Correlations among the b_f and b_{P_1} parameters.

	$b_{P_1}^1$	$b_{P_1}^2$	$b_{P_1}^3$	$b_{P_1}^4$	$b_{P_1}^5$	$b_{P_1}^6$	$b_{P_1}^7$	$b_{P_1}^8$	$b_{P_1}^9$	$b_{P_1}^{10}$
b_f^1	0.61	0.61	0.6	0.59	0.57	0.55	0.52	0.5	0.47	0.44
b_f^2	0.61	0.61	0.61	0.6	0.59	0.57	0.55	0.53	0.51	0.49
b_f^3	0.54	0.55	0.55	0.55	0.54	0.54	0.52	0.51	0.49	0.48
b_f^4	0.46	0.47	0.48	0.48	0.48	0.48	0.47	0.46	0.45	0.44
b_f^5	0.4	0.41	0.42	0.42	0.43	0.43	0.42	0.42	0.41	0.4
b_f^6	0.34	0.35	0.37	0.37	0.38	0.38	0.38	0.38	0.38	0.37
b_f^7	0.3	0.31	0.33	0.33	0.34	0.35	0.35	0.35	0.35	0.35
b_f^8	0.27	0.28	0.29	0.3	0.31	0.32	0.32	0.33	0.33	0.32
b_f^9	0.24	0.25	0.27	0.28	0.29	0.3	0.3	0.31	0.31	0.31
b_f^{10}	0.22	0.23	0.25	0.26	0.27	0.28	0.28	0.29	0.29	0.29

TABLE XXXIII. Correlations among the b_g and b_g parameters.

	b_g^1	b_g^2	b_g^3	b_g^4	b_g^5	b_g^6	b_g^7	b_g^8	b_g^9	b_g^{10}
b_g^1	1.0	0.99	0.98	0.96	0.92	0.88	0.84	0.79	0.75	0.7
b_g^2	0.99	1.0	0.99	0.98	0.96	0.93	0.89	0.85	0.81	0.77
b_g^3	0.98	0.99	1.0	1.0	0.98	0.96	0.93	0.9	0.87	0.83
b_g^4	0.96	0.98	1.0	1.0	1.0	0.98	0.96	0.94	0.91	0.88
b_g^5	0.92	0.96	0.98	1.0	1.0	1.0	0.98	0.97	0.95	0.92
b_g^6	0.88	0.93	0.96	0.98	1.0	1.0	1.0	0.99	0.97	0.95
b_g^7	0.84	0.89	0.93	0.96	0.98	1.0	1.0	1.0	0.99	0.98
b_g^8	0.79	0.85	0.9	0.94	0.97	0.99	1.0	1.0	1.0	0.99
b_g^9	0.75	0.81	0.87	0.91	0.95	0.97	0.99	1.0	1.0	1.0
b_g^{10}	0.7	0.77	0.83	0.88	0.92	0.95	0.98	0.99	1.0	1.0

TABLE XXXIV. Correlations among the b_g and $b_{\mathcal{F}_1}$ parameters.

	$b_{\mathcal{F}_1}^1$	$b_{\mathcal{F}_1}^2$	$b_{\mathcal{F}_1}^3$	$b_{\mathcal{F}_1}^4$	$b_{\mathcal{F}_1}^5$	$b_{\mathcal{F}_1}^6$	$b_{\mathcal{F}_1}^7$	$b_{\mathcal{F}_1}^8$	$b_{\mathcal{F}_1}^9$	$b_{\mathcal{F}_1}^{10}$
b_g^1	0.14	0.21	0.26	0.29	0.31	0.32	0.33	0.33	0.33	0.32
b_g^2	0.14	0.21	0.26	0.29	0.31	0.33	0.33	0.33	0.33	0.32
b_g^3	0.13	0.21	0.26	0.29	0.31	0.32	0.33	0.33	0.33	0.32
b_g^4	0.13	0.2	0.26	0.29	0.31	0.32	0.33	0.33	0.32	0.32
b_g^5	0.12	0.2	0.25	0.28	0.3	0.31	0.32	0.32	0.32	0.31
b_g^6	0.12	0.19	0.24	0.27	0.29	0.3	0.31	0.31	0.31	0.3
b_g^7	0.11	0.18	0.23	0.26	0.28	0.29	0.3	0.3	0.3	0.29
b_g^8	0.11	0.17	0.22	0.25	0.27	0.28	0.29	0.29	0.28	0.28
b_g^9	0.1	0.17	0.21	0.24	0.26	0.27	0.27	0.27	0.27	0.26
b_g^{10}	0.09	0.16	0.2	0.23	0.24	0.25	0.26	0.26	0.26	0.25

TABLE XXXV. Correlations among the b_g and b_{P_1} parameters.

	$b_{P_1}^1$	$b_{P_1}^2$	$b_{P_1}^3$	$b_{P_1}^4$	$b_{P_1}^5$	$b_{P_1}^6$	$b_{P_1}^7$	$b_{P_1}^8$	$b_{P_1}^9$	$b_{P_1}^{10}$
b_g^1	0.42	0.42	0.41	0.4	0.39	0.38	0.37	0.35	0.33	0.32
b_g^2	0.42	0.42	0.41	0.41	0.4	0.38	0.37	0.35	0.34	0.32
b_g^3	0.41	0.41	0.41	0.4	0.39	0.38	0.37	0.35	0.34	0.32
b_g^4	0.4	0.4	0.4	0.39	0.39	0.37	0.36	0.35	0.33	0.31
b_g^5	0.39	0.39	0.39	0.38	0.38	0.36	0.35	0.34	0.32	0.31
b_g^6	0.38	0.38	0.37	0.37	0.36	0.35	0.34	0.33	0.31	0.3
b_g^7	0.36	0.36	0.36	0.35	0.35	0.34	0.33	0.32	0.3	0.29
b_g^8	0.34	0.34	0.34	0.34	0.33	0.32	0.31	0.3	0.29	0.28
b_g^9	0.32	0.32	0.32	0.32	0.31	0.31	0.3	0.29	0.28	0.26
b_g^{10}	0.3	0.31	0.31	0.3	0.3	0.29	0.28	0.27	0.26	0.25

TABLE XXXVI. Correlations among the $b_{\mathcal{F}_1}$ and $b_{\mathcal{F}_1}$ parameters.

	$b_{\mathcal{F}_1}^1$	$b_{\mathcal{F}_1}^2$	$b_{\mathcal{F}_1}^3$	$b_{\mathcal{F}_1}^4$	$b_{\mathcal{F}_1}^5$	$b_{\mathcal{F}_1}^6$	$b_{\mathcal{F}_1}^7$	$b_{\mathcal{F}_1}^8$	$b_{\mathcal{F}_1}^9$	$b_{\mathcal{F}_1}^{10}$
$b_{\mathcal{F}_1}^1$	1.0	0.95	0.86	0.76	0.68	0.61	0.55	0.5	0.46	0.42
$b_{\mathcal{F}_1}^2$	0.95	1.0	0.97	0.92	0.86	0.8	0.75	0.69	0.64	0.58
$b_{\mathcal{F}_1}^3$	0.86	0.97	1.0	0.98	0.95	0.91	0.87	0.82	0.76	0.7
$b_{\mathcal{F}_1}^4$	0.76	0.92	0.98	1.0	0.99	0.97	0.93	0.89	0.84	0.79
$b_{\mathcal{F}_1}^5$	0.68	0.86	0.95	0.99	1.0	0.99	0.97	0.94	0.9	0.85
$b_{\mathcal{F}_1}^6$	0.61	0.8	0.91	0.97	0.99	1.0	0.99	0.97	0.95	0.9
$b_{\mathcal{F}_1}^7$	0.55	0.75	0.87	0.93	0.97	0.99	1.0	0.99	0.98	0.95
$b_{\mathcal{F}_1}^8$	0.5	0.69	0.82	0.89	0.94	0.97	0.99	1.0	0.99	0.98
$b_{\mathcal{F}_1}^9$	0.46	0.64	0.76	0.84	0.9	0.95	0.98	0.99	1.0	0.99
$b_{\mathcal{F}_1}^{10}$	0.42	0.58	0.7	0.79	0.85	0.9	0.95	0.98	0.99	1.0

TABLE XXXVII. Correlations among the b_{F_1} and b_{P_1} parameters.

	$b_{P_1}^1$	$b_{P_1}^2$	$b_{P_1}^3$	$b_{P_1}^4$	$b_{P_1}^5$	$b_{P_1}^6$	$b_{P_1}^7$	$b_{P_1}^8$	$b_{P_1}^9$	$b_{P_1}^{10}$
$b_{F_1}^1$	0.57	0.56	0.55	0.54	0.52	0.5	0.48	0.46	0.43	0.4
$b_{F_1}^2$	0.71	0.71	0.71	0.7	0.69	0.67	0.65	0.63	0.61	0.58
$b_{F_1}^3$	0.78	0.79	0.79	0.79	0.79	0.78	0.76	0.74	0.72	0.7
$b_{F_1}^4$	0.81	0.83	0.84	0.84	0.84	0.84	0.83	0.81	0.79	0.77
$b_{F_1}^5$	0.82	0.84	0.86	0.87	0.87	0.87	0.87	0.85	0.84	0.82
$b_{F_1}^6$	0.82	0.85	0.87	0.88	0.89	0.89	0.89	0.88	0.86	0.85
$b_{F_1}^7$	0.82	0.85	0.87	0.89	0.9	0.9	0.9	0.89	0.88	0.86
$b_{F_1}^8$	0.8	0.83	0.86	0.88	0.89	0.9	0.9	0.89	0.88	0.87
$b_{F_1}^9$	0.78	0.81	0.84	0.86	0.87	0.88	0.88	0.88	0.87	0.86
$b_{F_1}^{10}$	0.75	0.78	0.81	0.83	0.85	0.86	0.86	0.86	0.85	0.84

TABLE XXXVIII. Correlations among the b_{P_1} and b_{P_1} parameters.

	$b_{P_1}^1$	$b_{P_1}^2$	$b_{P_1}^3$	$b_{P_1}^4$	$b_{P_1}^5$	$b_{P_1}^6$	$b_{P_1}^7$	$b_{P_1}^8$	$b_{P_1}^9$	$b_{P_1}^{10}$
$b_{P_1}^1$	1.0	1.0	0.99	0.97	0.94	0.91	0.88	0.84	0.8	0.76
$b_{P_1}^2$	1.0	1.0	1.0	0.99	0.97	0.94	0.92	0.88	0.85	0.81
$b_{P_1}^3$	0.99	1.0	1.0	1.0	0.99	0.97	0.95	0.92	0.89	0.86
$b_{P_1}^4$	0.97	0.99	1.0	1.0	1.0	0.99	0.97	0.95	0.93	0.9
$b_{P_1}^5$	0.94	0.97	0.99	1.0	1.0	1.0	0.99	0.97	0.95	0.93
$b_{P_1}^6$	0.91	0.94	0.97	0.99	1.0	1.0	1.0	0.99	0.97	0.96
$b_{P_1}^7$	0.88	0.92	0.95	0.97	0.99	1.0	1.0	1.0	0.99	0.98
$b_{P_1}^8$	0.84	0.88	0.92	0.95	0.97	0.99	1.0	1.0	1.0	0.99
$b_{P_1}^9$	0.8	0.85	0.89	0.93	0.95	0.97	0.99	1.0	1.0	1.0
$b_{P_1}^{10}$	0.76	0.81	0.86	0.9	0.93	0.96	0.98	0.99	1.0	1.0

-
- [1] D. Bigi and P. Gambino, Revisiting $B \rightarrow D \ell \nu$, Phys. Rev. D **94**, 094008 (2016).
- [2] F. U. Bernlochner, Z. Ligeti, M. Papucci, and D. J. Robinson, Combined analysis of semileptonic B decays to D and D^* : $R(D^{(*)})$, $|V_{cb}|$, and new physics, Phys. Rev. D **95**, 115008 (2017); **97**, 059902(E) (2018).
- [3] S. Jaiswal, S. Nandi, and S. K. Patra, Extraction of $|V_{cb}|$ from $B \rightarrow D^{(*)} \ell \nu_\ell$ and the Standard Model predictions of $R(D^{(*)})$, J. High Energy Phys. 12 (2017) 060.
- [4] F. U. Bernlochner, Z. Ligeti, and D. J. Robinson, $N = 5, 6, 7, 8$: Nested hypothesis tests and truncation dependence of $|V_{cb}|$, Phys. Rev. D **100**, 013005 (2019).
- [5] P. Gambino, M. Jung, and S. Schacht, The V_{cb} puzzle: An update Phys. Lett. B **795**, 386 (2019).
- [6] M. Bordone, M. Jung, and D. van Dyk, Theory determination of $\bar{B} \rightarrow D^{(*)} \ell^- \bar{\nu}$ form factors at $\mathcal{O}(1/m_c^2)$, Eur. Phys. J. C **80**, 74 (2020).
- [7] S. Jaiswal, S. Nandi, and S. K. Patra, Updates on extraction of $|V_{cb}|$ and SM prediction of $R(D^*)$ in $B \rightarrow D^* \ell \nu_\ell$ decays, J. High Energy Phys. 06 (2020) 165.
- [8] G. Martinelli, S. Simula, and L. Vittorio, $|V_{cb}|$ and $R(D^{(*)})$ using lattice QCD and unitarity, Phys. Rev. D **105**, 034503 (2022).
- [9] F. U. Bernlochner, Z. Ligeti, M. Papucci, M. T. Prim, D. J. Robinson, and C. Xiong, Constrained

- second-order power corrections in HQET: $R(D^{(*)})$, $|V_{cb}|$, and new physics, *Phys. Rev. D* **106**, 096015 (2022).
- [10] A. Biswas, S. Nandi, and I. Ray, Extractions of $|V_{ub}|/|V_{cb}|$ from a combined study of the exclusive $b \rightarrow u(c)\ell\nu_\ell$ decays, *J. High Energy Phys.* **07** (2023) 024.
- [11] B.-Y. Cui, Y.-K. Huang, Y.-M. Wang, and X.-C. Zhao, Shedding new light on $\mathcal{R}(D_{(s)}^{(*)})$ and $|V_{cb}|$ from semileptonic $\bar{B}_{(s)} \rightarrow D_{(s)}^{(*)}\ell\bar{\nu}_\ell$ decays, [arXiv:2301.12391](https://arxiv.org/abs/2301.12391).
- [12] Y. Amhis *et al.* (HFLAV Collaboration), Averages of b -hadron, c -hadron, and τ -lepton properties as of 2021, *Phys. Rev. D* **107**, 052008 (2023) and updated results and plots available at <https://hflav-eos.web.cern.ch/hflav-eos/semi/fall22/html/RDsDsstar/RDRDs.html>.
- [13] Y. Aoki *et al.* (FLAG Collaboration), FLAG review 2021, *Eur. Phys. J. C* **82**, 869 (2022).
- [14] M. Bona *et al.* (UTfit Collaboration), New UTfit analysis of the unitarity triangle in the Cabibbo-Kobayashi-Maskawa scheme, *Rend. Fis. Acc. Lincei* **34**, 37 (2023).
- [15] W. Qian *et al.* (CKMfitter Collaboration), Recent CKMfitter updates on global fits of the CKM matrix, <https://indico.cern.ch/event/891123/contributions/4601722/attachments/2351890/4013122/CKMfitter2021.pdf>.
- [16] A. Crivellin and S. Pokorski, Can the Differences in the Determinations of V_{ub} and V_{cb} be Explained by New Physics?, *Phys. Rev. Lett.* **114**, 011802 (2015).
- [17] M. Jung and D. M. Straub, Constraining new physics in $b \rightarrow c\ell\nu$ transitions, *J. High Energy Phys.* **01** (2019) 009.
- [18] S. Iguro and R. Watanabe, Bayesian fit analysis to full distribution data of $\bar{B} \rightarrow D^{(*)}\ell\bar{\nu}:|V_{cb}|$ determination and new physics constraints, *J. High Energy Phys.* **08** (2020) 006.
- [19] A. Crivellin, Effects of right-handed charged currents on the determinations of $|V(ub)|$ and $|V(cb)|$, *Phys. Rev. D* **81**, 031301 (2010).
- [20] P. Ball, $V(cb)$ from semileptonic B decays and the reliability of the infinite quark mass limit, *Phys. Lett. B* **281**, 133 (1992).
- [21] N. Gubernari, A. Kokulu, and D. van Dyk, $B \rightarrow P$ and $B \rightarrow V$ form factors from B -meson light-cone sum rules beyond leading twist, *J. High Energy Phys.* **01** (2019) 150.
- [22] A. Bazavov *et al.* (Fermilab Lattice and MILC Collaborations), Semileptonic form factors for $B \rightarrow D^*\ell\nu$ at nonzero recoil from 2 + 1-flavor lattice QCD, *Eur. Phys. J. C* **82**, 1141 (2022); **83**, 21(E) (2023).
- [23] J. Harrison and C. T. H. Davies, $B \rightarrow D^*$ vector, axial-vector and tensor form factors for the full q^2 range from lattice QCD, [arXiv:2304.03137](https://arxiv.org/abs/2304.03137).
- [24] J. P. Lees *et al.* (BABAR Collaboration), Evidence for an Excess of $\bar{B} \rightarrow D^{(*)}\tau^-\bar{\nu}_\tau$ Decays, *Phys. Rev. Lett.* **109**, 101802 (2012).
- [25] J. P. Lees *et al.* (BABAR Collaboration), Measurement of an Excess of $\bar{B} \rightarrow D^{(*)}\tau^-\bar{\nu}_\tau$ Decays and Implications for Charged Higgs Bosons, *Phys. Rev. D* **88**, 072012 (2013).
- [26] M. Huschle *et al.* (Belle Collaboration), Measurement of the branching ratio of $\bar{B} \rightarrow D^{(*)}\tau^-\bar{\nu}_\tau$ relative to $\bar{B} \rightarrow D^{(*)}\ell^-\bar{\nu}_\ell$ decays with hadronic tagging at Belle, *Phys. Rev. D* **92**, 072014 (2015).
- [27] Y. Sato *et al.* (Belle Collaboration), Measurement of the branching ratio of $\bar{B}^0 \rightarrow D^{*+}\tau^-\bar{\nu}_\tau$ relative to $\bar{B}^0 \rightarrow D^{*+}\ell^-\bar{\nu}_\ell$ decays with a semileptonic tagging method, *Phys. Rev. D* **94**, 072007 (2016).
- [28] Y. Sato *et al.* (Belle Collaboration), Measurement of the τ Lepton Polarization and $R(D^*)$ in the Decay $\bar{B} \rightarrow D^*\tau^-\bar{\nu}_\tau$, *Phys. Rev. Lett.* **118**, 211801 (2017).
- [29] S. Hirose *et al.* (Belle Collaboration), Measurement of the τ lepton polarization and $R(D^*)$ in the decay $\bar{B} \rightarrow D^*\tau^-\bar{\nu}_\tau$ with one-prong hadronic τ decays at Belle, *Phys. Rev. D* **97**, 012004 (2018).
- [30] G. Caria *et al.* (Belle Collaboration), Measurement of $\mathcal{R}(D)$ and $\mathcal{R}(D^*)$ with a Semileptonic Tagging Method, *Phys. Rev. Lett.* **124**, 161803 (2020).
- [31] R. Aaij *et al.* (LHCb Collaboration), Measurement of the Ratio of Branching Fractions $\mathcal{B}(\bar{B}^0 \rightarrow D^{*+}\tau^-\bar{\nu}_\tau)/\mathcal{B}(\bar{B}^0 \rightarrow D^{*+}\mu^-\bar{\nu}_\mu)$, *Phys. Rev. Lett.* **115**, 111803 (2015); **115**, 159901(E) (2015).
- [32] R. Aaij *et al.* (LHCb Collaboration), Measurement of the Ratio of the $B^0 \rightarrow D^{*-}\tau^+\nu_\tau$ and $B^0 \rightarrow D^{*-}\mu^+\nu_\mu$ Branching Fractions Using Three-Prong τ -Lepton Decays, *Phys. Rev. Lett.* **120**, 171802 (2018).
- [33] R. Aaij *et al.* (LHCb Collaboration), Test of lepton flavor universality by the measurement of the $B^0 \rightarrow D^{*-}\tau^+\nu_\tau$ branching fraction using three-prong τ decays, *Phys. Rev. D* **97**, 072013 (2018).
- [34] R. Aaij *et al.* (LHCb Collaboration), First joint measurement of $R(D^*)$ and $R(D^0)$ at LHCb, <https://indico.cern.ch/event/1187939/>.
- [35] M. Di Carlo *et al.*, Unitarity bounds for semileptonic decays in lattice QCD, *Phys. Rev. D* **104**, 054502 (2021).
- [36] G. Martinelli, S. Simula, and L. Vittorio, Constraints for the semileptonic $B \rightarrow D^{(*)}$ form factors from lattice QCD simulations of two-point correlation functions, *Phys. Rev. D* **104**, 094512 (2021).
- [37] G. Martinelli, S. Simula, and L. Vittorio, Exclusive determinations of $|V_{cb}|$ and $R(D^*)$ through unitarity, *Eur. Phys. J. C* **82**, 1083 (2022).
- [38] G. Martinelli, M. Naviglio, S. Simula, and L. Vittorio, $|V_{cb}|$, lepton flavor universality and SU(3)F symmetry breaking in $B_s \rightarrow D_s^{(*)}\ell\nu_\ell$ decays through unitarity and lattice QCD, *Phys. Rev. D* **106**, 093002 (2022).
- [39] M. Bordone, B. Capdevila, and P. Gambino, Three loop calculations and inclusive V_{cb} , *Phys. Lett. B* **822**, 136679 (2021).
- [40] F. Bernlochner, M. Fael, K. Olschewsky, E. Persson, R. van Tonder, K. Keri Vos, and M. Welsch, First extraction of inclusive V_{cb} from q^2 moments, *J. High Energy Phys.* **10** (2022) 068.
- [41] M. T. Prim *et al.* (Belle Collaboration), Measurement of differential distributions of $B \rightarrow D^*\ell\bar{\nu}_\ell$ and implications on $|V_{cb}|$, *Phys. Rev. D* **108**, 012002 (2023).
- [42] C. Lyu *et al.* (Belle II Collaboration), Recent semileptonic results from Belle II, <https://indico.cern.ch/event/1204084/contributions/5298272/>.
- [43] C. G. Boyd, B. Grinstein, and R. F. Lebed, Model independent extraction of $|V(cb)|$ using dispersion relations, *Phys. Lett. B* **353**, 306 (1995).
- [44] C. G. Boyd, B. Grinstein, and R. F. Lebed, Model independent determinations of anti- $B \rightarrow D$ (lepton), D^* (lepton) anti-neutrino form-factors, *Nucl. Phys.* **B461**, 493 (1996).
- [45] C. G. Boyd, B. Grinstein, and R. F. Lebed, Precision corrections to dispersive bounds on form-factors, *Phys. Rev. D* **56**, 6895 (1997).

- [46] I. Caprini, L. Lellouch, and M. Neubert, Dispersive bounds on the shape of $\bar{B} \rightarrow D^{(*)}\ell\bar{\nu}$ form-factors, *Nucl. Phys.* **B530**, 153 (1998).
- [47] N. Isgur and M. B. Wise, Weak decays of heavy mesons in the static quark approximation, *Phys. Lett. B* **232**, 113 (1989).
- [48] M. Neubert, Heavy quark symmetry, *Phys. Rep.* **245**, 259 (1994).
- [49] D. Bigi, P. Gambino, and S. Schacht, A fresh look at the determination of $|V_{cb}|$ from $B \rightarrow D^*\ell\nu$, *Phys. Lett. B* **769**, 441 (2017).
- [50] D. Bigi, P. Gambino, and S. Schacht, $R(D^*)$, $|V_{cb}|$, and the heavy quark symmetry relations between form factors, *J. High Energy Phys.* **11** (2017) 061.
- [51] J. M. Flynn, A. Jüttner, and J. T. Tsang, Bayesian inference for form-factor fits regulated by unitarity and analyticity, [arXiv:2303.11285](#).
- [52] A. F. Falk and M. Neubert, Second order power corrections in the heavy quark effective theory. 1. Formalism and meson form-factors, *Phys. Rev. D* **47**, 2965 (1993).
- [53] M. Neubert, Z. Ligeti, and Y. Nir, QCD sum rule analysis of the subleading Isgur-Wise form-factor $\chi_2(v \cdot v')$, *Phys. Lett. B* **301**, 101 (1993).
- [54] M. Neubert, Z. Ligeti, and Y. Nir, The subleading Isgur-Wise form-factor $\chi_3(v \cdot v')$ to order α_s in QCD sum rules, *Phys. Rev. D* **47**, 5060 (1993).
- [55] Z. Ligeti, Y. Nir, and M. Neubert, Subleading Isgur-Wise form-factor $\xi_3(v \cdot v')$ and its implications for the decays $\bar{B} \rightarrow D^{(*)}\ell\bar{\nu}$, *Phys. Rev. D* **49**, 1302 (1994).
- [56] G. Martinelli, S. Simula, and L. Vittorio, Exclusive semi-leptonic $B \rightarrow \pi\ell\nu_\ell$ and $B_s \rightarrow K\ell\nu_\ell$ decays through unitarity and lattice QCD, *J. High Energy Phys.* **08** (2022) 022.
- [57] C. G. Boyd, B. Grinstein, and R. F. Lebed, Constraints on Form-Factors for Exclusive Semileptonic Heavy to Light Meson Decays, *Phys. Rev. Lett.* **74**, 4603 (1995).
- [58] C. Bourrely, B. Machet, and E. de Rafael, Semileptonic decays of pseudoscalar particles ($M \rightarrow M'\ell\nu_\ell$) and short distance behavior of quantum chromodynamics, *Nucl. Phys. B* **189**, 157 (1981).
- [59] L. Lellouch, Lattice constrained unitarity bounds for $B^0 \rightarrow \pi^+\ell^-\bar{\nu}_\ell$ decays, *Nucl. Phys.* **B479**, 353 (1996).
- [60] J. De Blas *et al.*, HEPfit: A code for the combination of indirect and direct constraints on high energy physics models, *Eur. Phys. J. C* **80**, 456 (2020).
- [61] S. Hirose *et al.* (Belle Collaboration), Measurement of the τ Lepton Polarization and $R(D^*)$ in the Decay $\bar{B} \rightarrow D^*\tau^-\bar{\nu}_\tau$, *Phys. Rev. Lett.* **118**, 211801 (2017).
- [62] A. Abdesselam *et al.*, on behalf of Belle Collaboration, Measurement of the D^{*-} polarization in the decay $B^0 \rightarrow D^{*-}\tau^+\nu_\tau$, in *Proceedings of the 10th International Workshop on the CKM Unitarity Triangle*, 2019, [arXiv:1903.03102](#).
- [63] A. Abdesselam *et al.* (Belle Collaboration), Precise determination of the CKM matrix element $|V_{cb}|$ with $\bar{B}^0 \rightarrow D^{*+}\ell^-\bar{\nu}_\ell$ decays with hadronic tagging at Belle, [arXiv:1702.01521](#).
- [64] E. Waheed *et al.* (Belle Collaboration), Measurement of the CKM matrix element $|V_{cb}|$ from $B^0 \rightarrow D^{*-}\ell^+\nu_\ell$ at Belle, *Phys. Rev. D* **100**, 052007 (2019); **103**, 079901(E) (2021).
- [65] L. Vittorio, The D(M)M perspective on Flavour Physics, Ph.D. thesis, Pisa, Scuola Normale Superiore, 2022.
- [66] S. Fajfer, J. F. Kamenik, I. Nisandzic, and J. Zupan, Implications of Lepton Flavor Universality Violations in B Decays, *Phys. Rev. Lett.* **109**, 161801 (2012).
- [67] A. Crivellin, C. Greub, and A. Kokulu, Explaining $B \rightarrow D\tau\nu$, $B \rightarrow D^*\tau\nu$ and $B \rightarrow \tau\nu$ in a 2HDM of type III, *Phys. Rev. D* **86**, 054014 (2012).
- [68] P. Colangelo and F. De Fazio, Scrutinizing $\bar{B} \rightarrow D^*(D\pi)\ell^-\bar{\nu}_\ell$ and $\bar{B} \rightarrow D^*(D\gamma)\ell^-\bar{\nu}_\ell$ in search of new physics footprints, *J. High Energy Phys.* **06** (2018) 082.
- [69] A. Carvunis, A. Crivellin, D. Guadagnoli, and S. Gangal, The forward-backward asymmetry in $B \rightarrow D^*\ell\nu$: One more hint for scalar leptoquarks?, *Phys. Rev. D* **105**, L031701 (2022).
- [70] A. Azatov, D. Bardhan, D. Ghosh, F. Sgarlata, and E. Venturini, Anatomy of $b \rightarrow c\tau\nu$ anomalies, *J. High Energy Phys.* **11** (2018) 187.
- [71] S. Iguro, T. Kitahara, and R. Watanabe, Global fit to $b \rightarrow c\tau\nu$ anomalies 2022 mid-autumn, [arXiv:2210.10751](#).
- [72] G. Aad *et al.* (ATLAS Collaboration), Search for a heavy charged boson in events with a charged lepton and missing transverse momentum from pp collisions at $\sqrt{s} = 13$ TeV with the ATLAS detector, *Phys. Rev. D* **100**, 052013 (2019).
- [73] S. Iguro, M. Takeuchi, and R. Watanabe, Testing leptoquark/EFT in $\bar{B} \rightarrow D^{(*)}\bar{\nu}$ at the LHC, *Eur. Phys. J. C* **81**, 406 (2021).
- [74] M. Fedele, M. Blanke, A. Crivellin, S. Iguro, T. Kitahara, U. Nierste, and R. Watanabe, Impact of $\Lambda_b \rightarrow \Lambda_c\tau\nu$ measurement on new physics in $b \rightarrow c\ell\nu$ transitions, *Phys. Rev. D* **107**, 055005 (2023).
- [75] I. Ray and S. Nandi, Test of new physics effects in $\bar{B} \rightarrow (D^{(*)}, \pi)\ell^-\bar{\nu}_\ell$ decays with heavy and light leptons, [arXiv:2305.11855](#).